COO-3130TB-214

# PROGRESS REPORT OF A RESEARCH PROGRAM IN EXPERIMENTAL HIGH ENERGY PHYSICS

Progress Report

Anatole M. Shapiro and Robert E. Lanou, Jr.

Brown University
Providence, Rhode Island



September 1, 1974 - August 31, 1975

PREPARED FOR THE U.S. ENERGY RESEARCH AND DEVELOPMENT ADMINISTRATION
UNDER CONTRACT NO. E(11-1)-3130 (TASK B-EXPERIMENTAL)

# DISCLAIMER

## ABSTRACT

An experimental program in strong interaction physics is being carried out using bubble chamber-hybrid system and counter-spark chamber techniques. The experiments have been and are being performed utilizing the accelerators of the National Laboratories at Argonne, Brookhaven, and Batavia.

In 4.1 GeV/c $\pi^+p$ interactions, the bubble chamber group is studying: 1) $\pi^+$ and $\pi^-$ inclusive distributions; 2) two-particle correlations; 3) two-body and quasi-two-body production mechanisms; and 4) strange-particle production. A multiwire proportional hybrid system has been brought into operation at FNAL. With it, aspects of 150 GeV/c $\pi^-p$, $\pi^+p$, and pp interactions are being studied: 1) total and partial cross sections; 2) charged-particle multiplicity distributions and their moments; 3) single-particle inclusive distributions and two-particle correlations; 4) leading particle and diffraction phenomena; and 5) production models for high-multiplicity events.

The experiments of the counter-spark chamber group include the following: 1) a study of baryon exchange processes using backward pion charge exchange; 2) a search for high mass boson resonances and the determination of their quantum numbers in antiproton-proton systems; 3) a nucleon-nucleon and meson-nucleon elastic and quasi-elastic scattering experiment at the highest accelerator energies possible; protons, pions and kaons are used as projectiles and protons and neutrons as targets; the role of the pomeron and exchange models generally is being investigated; and 4) a measurement of the inclusive spectra of hadrons as a function of multiplicity at FNAL energies.

## Legal Notice

"This report was prepared as an account of Government-sponsored work. Neither the United States, nor the Energy Research and Development Administration nor any person acting on behalf of the Administration:

A. Makes any warranty or representation, expressed or implied, with respect to the accuracy, completeness, or usefulness of the information contained in this report, or that the use of any information, apparatus, method or process disclosed in this report may not infringe privately owned rights; or

B. Assumes any liabilities with respect to the use of, or for damages resulting from the use of, any information, apparatus, method, or process disclosed in this report.

As used in the above, 'person acting on behalf of the Administration' includes any employee or contractor of the Administration, or employee of such contractor, to the extent that such employee or contractor of the Administration, or employee of such contractor prepares, disseminates, or provides access to, any information pursuant to his employment or contract with the Administration, or his employment with such contractor."

# Progress Report of a Research Program in Experimental High Energy Physics

The Department of Physics of Brown University presents herein a report of the progress made in the experimental program during the present contract year (1 September 1974 - 31 August 1975). This work has been supported by the U.S. Energy Research and Development Administration under Contract E(11-1)-3130 (Task B-Experimental).

This report is divided as follows:

A. Bubble Chamber-Proportional Hybrid System Program.

I. Data Analysis in Progress.

a) The Argonne $\pi^+p$ Bubble Chamber Experiment - First Stage.

Results of this experiment have been discussed in detail in earlier Progress Reports and a number of papers on this work have been published. These include a study of inclusive production of $\pi^+$, $\pi^-$, and $2\pi^-$, and correlations among the produced pions;[1] and results of the analysis of exclusive events identified as $\pi^+p \rightarrow$ four charged particles + neutrals,[2] as well as several talks at American Physical Society meetings. A paper is now being prepared on the production of $\rho$ mesons and $\Delta^{++}$ hyperons in two- and four-prong interactions:

$$\pi^+p \rightarrow \Delta^{++}\pi^\circ \rightarrow p\pi^+\pi^\circ \quad ,$$

$$\pi^+p \rightarrow p\rho^+ \rightarrow p\pi^+\pi^\circ \quad ,$$

$$\pi^+p \rightarrow \Delta^{++}\rho^\circ \rightarrow p\pi^+\pi^+\pi^- \quad ,$$

$$\pi^+p \rightarrow p\pi^+\rho^\circ \rightarrow p\pi^+\pi^+\pi^- \quad .$$

The first two interactions each account for about 10 percent of the cross section for the production of the final state $p\pi^+\pi^\circ$, while the last two account for about 8 percent and 30 percent of the final state $p\pi^+\pi^+\pi^-$, respectively.

---

1. D. G. Fong, A. M. Shapiro, and M. Widgoff, Phys. Rev. D8, 3765 (1973).
2. D. G. Fong et al., Phys. Rev. D9, 3015 (1974).

b) The Argonne $\pi^+p$ Bubble Chamber Experiment - Second Stage.

This second stage of the experiment on $\pi^+p$ interactions at 4.1 GeV/c is based on 395,000 good pictures, taken in addition to the 100,000 of the first stage. As reported last year, these pictures have been scanned for all $\pi^+p$ events occurring within a central fiducial volume. About 15% of the film has been double scanned in order to measure the scanning efficiencies for the various topologies observed. About 90,000 events have been found in all, with topologies as given below:

| Topology | Events on Film |
|---|---|
| 2 Prong | 51,400 |
| 4 Prong | 35,900 |
| >4 Prong | 2,400 |

The measurements on this film have been carried out in two passes. In the first pass all four-prong events and two-prong events having one or more associated V°'s were measured, mainly using the MIT PEPR system after pre-digitizing at Brown. All strange-particle production in this sample was studied by Dr. R. Simard as part of his Ph.D. dissertation. He obtained cross sections for thirty-six different final states involving strange particles (see Section C, Reference 194).

Approximately 15% of this sample was judged not suitable for PEPR and another 15% was not well-measured by PEPR. These have been hand-measured at Brown on our Hermes and Franckenstein machines. Ionization estimates are being added to the last of these events and then the TVGP and SQUAW calculations will be completed.

In the second pass the remaining two-prong, six-prong and eight-prong events are being measured. The pre-digitizing of these events at Brown is 98% completed and the PEPR measurements are in progress. When the calculations are done, we shall be able to conclude our study of strange-particle production and to extend the analyses discussed in the preceding section with five times the statistics of the first stage.

### (c) The Proportional Hybrid System (PHS) Experiment at FNAL (FNAL Experiment #154).

The testing of the entire PHS, including the bubble chamber and up-stream and downstream proportional wire counters and the upstream Cerenkov counter, was described in the Progress Report of June 1974. The success-ful linking of signals in the counters with bubble chamber tracks was described in that Report, and in several talks at the January 1974 Annual Meeting of the American Physical Society.[3] The concluding stage in this experiment is the analysis of a 109,000-frame exposure of $\pi^-$ mesons at a momentum of 147 GeV/c, obtained in March 1974.

The PHS Consortium, as previously planned, divided the film among several institutions for scanning and predigitizing. These institutions are Brown, IIT, Johns Hopkins, MIT, Oak Ridge-Tennessee, Rutgers-Stevens, and Yale-FNAL. All the data were put into compatible format for processing by the MIT PEPR system, through which all the film has now passed. The post-PEPR analysis program GEOMAT[3] (a track-matching three-view geometrical reconstruction program for bubble chamber measurements) and TRACK ORGANIZER (a program for linking bubble chamber track measurements to PWC track measurements, developed at Brown -- see Section C, Reference 195) have

3. E. S. Hafen et al., B.A.P.S. 19, 96 (1974).
W. Bugg et al., B.A.P.S. 19, 96 (1974).
T. Ludlam et al., B.A.P.S. 19, 96 (1974).
T. L. Watts et al., B.A.P.S. 19, 96 (1974).

yielded a high percentage of successful track reconstructions, as seen by careful visual comparison of computer results with the film. These programs, as well as the PEPR software programs and the PWC track reconstruction program PWGP are being refined on the basis of this experiment to yield still better results in following experiments.

In order to check on possible biases in the interpretation of results, events that were bypassed in the scanning as being unsuitable for PEPR, and events that failed reconstruction, are being measured by hand on precision measuring machines. This work has been divided among members of the Consortium, and Brown is working on the measurement of events with six or more prongs. This is usually a very complicated procedure, but our technicians are meeting this challenge very successfully.

Preliminary analysis of the experimental results has very promptly yielded interesting physics. A Physics Letter has been published, as well as four papers presented at the January 1975 meeting of the American Physical Society, and eight papers at the April 1975 meeting of the APS (see Section C, References 192, 196-209). Some of the results are briefly discussed here.

(i) Charged and Neutral Particle Multiplicity Distributions.

The charged particle multiplicity distribution as determined from analysis of about 40% of the film has been published (Reference 196), and is given in Table I. Moments of this multiplicity distribution are given in Table II, together with corresponding results at three other $\pi^-$ momenta

Table 1. Topological Cross Sections in 147 GeV/c $\pi^- p$ Interactions.

| Number of Prongs | Events Found | Corrected Number | Cross Section (mb) |
|---|---|---|---|
| 2 | 1276 | 1592 ± 52<br>elastic 952 ± 64<br>inelastic 640 ± 52 | 5.15 ± 0.17<br>elastic 3.08 ± 0.21<br>inelastic 2.07 ± 0.17 |
| 3 | 9 | | |
| 4 | 1194 | 1266 ± 40 | 4.10 ± 0.14 |
| 5 | 0 | | |
| 6 | 1351 | 1424 ± 40 | 4.61 ± 0.14 |
| 7 | 5 | | |
| 8 | 1299 | 1350 ± 38 | 4.37 ± 0.14 |
| 9 | 16 | | |
| 10 | 939 | 970 ± 33 | 3.14 ± 0.11 |
| 11 | 4 | | |
| 12 | 526 | 536 ± 25 | 1.74 ± 0.08 |
| 13 | 9 | | |
| 14 | 244 | 251 ± 17 | 0.81 ± 0.06 |
| 15 | 2 | | |
| 16 | 114 | 115 ± 11 | 0.37 ± 0.04 |
| 17 | 5 | | |
| 18 | 50 | 51 ± 7 | 0.17 ± 0.02 |
| 19 | 0 | | |
| 20 | 26 | 26 ± 5 | 0.084 ± 0.016 |
| 21 | 0 | | |
| 22 | 4 | 4 ± 2 | 0.013 ± 0.006 |
| 23 | 0 | | |
| 24 | 1 | 1 ± 1 | 0.003 ± 0.003 |
| Total | 7074 | 7586 ± 92 | 24.6 ± 0.4 |

Table 2. Multiplicity Moments in Inelastic $\pi^- p$ Interactions.

| | 50 GeV/c [a] | 100 GeV/c [b] | 147 GeV/c | 205 GeV/c [c] |
|---|---|---|---|---|
| $\langle n \rangle$ | 5.78 ± 0.04 | 6.79 ± 0.08 | 7.34 ± 0.10 | 8.02 ± 0.12 |
| $\langle n(n-1) \rangle$ | 34.9 ± 0.48 | 49 ± 1 | 59.4 ± 1.1 | 71.6 ± 1.8 |
| $\langle n^2 \rangle$ | 40.7 ± 0.48 | 56 ± 1 | 66.7 ± 1.2 | 79.6 ± 1.8 |
| $f_2$ | 1.53 ± 0.15 | 3.2 ± 0.3 | 5.5 ± 0.5 | 7.24 ± 0.61 |
| D | 2.70 ± 0.03 | 3.16 ± 0.04 | 3.58 ± 0.05 | 3.91 ± 0.11 |
| $\langle n \rangle / D$ | 2.14 ± 0.03 | 2.15 ± 0.04 | 2.05 ± 0.04 | 2.05 ± 0.05 |

$f_2 = \langle n(n-1) \rangle - \langle n \rangle^2$ ; $D = (\langle n^2 \rangle - \langle n \rangle^2)^{1/2}$ .

a. G. A. Akopdjanov et al., Nucl. Phys. B75, 401 (1974).
b. E. L. Berger et al., Nucl. Phys. B77, 365 (1974).
c. D. Bogert et al., Phys. Rev. Letters 31, 1271 (1973).

- - - - - - - - - - - -

Table 3. Multiplicity Distributions for $\pi^- p \rightarrow \gamma + n_c$ + Anything.

| $n_c$ - No. of Charged Prongs | Number of Observed $\gamma$ | Corrected and Weighted Number | $\sigma_n(\gamma)$ (mb) | $\langle n_{\pi^0} \rangle$ per Inelastic Interaction |
|---|---|---|---|---|
| 2 | 22 | 2,982 | 5.8 ± 1.8 | 1.4 ± 0.4 |
| 4 | 81 | 10,407 | 20.2 ± 3.2 | 2.5 ± 0.4 |
| 6 | 102 | 13,030 | 25.3 ± 3.5 | 2.8 ± 0.4 |
| 8 | 122 | 15,619 | 30.3 ± 3.9 | 3.5 ± 0.5 |
| 10 | 86 | 12,144 | 23.6 ± 3.6 | 4.1 ± 0.6 |
| 12 | 46 | 6,185 | 12.0 ± 2.5 | 3.4 ± 0.7 |
| 14 | 13 | 1,584 | 3.1 ± 1.2 | 1.9 ± 0.8 |
| 16 | 2 | 300 | 0.6 | 0.8 |
| Total | 474 | 62,253 | 120.8 ± 6.0 | |

from other experiments. The values of the average charged-particle multiplicity for inelastic events $\langle n_c \rangle$ at the four beam momenta have been fitted to the formula

$$\langle n_c \rangle = a + b \ \ln (s/s_o) \ , \quad s_o = (1 \text{ GeV})^2 \quad .$$

We find a = −1.2 ± 0.3 and b = 1.54 ± 0.07, with a chi-squared value of 2.0 for two degrees of freedom, or a 35% confidence level. In addition, we find that the ratio of $\langle n_c \rangle$ to the dispersion D $(= (\langle n_c^2 \rangle - \langle n_c \rangle^2)^{1/2})$ varies only slightly over the whole multiplicity range. The ratio remains close to constant (∿2.1) for $\pi^- p$ interactions down to very low $\pi^-$ momenta,[4] and also for the very high multiplicities obtained in $\pi^-$ - nucleus interactions.[5] All these data give values of the dispersion D inconsistent with a Poisson distribution of particle multiplicities. Data for the whole experiment are now being analyzed, with very much improved information on corrections to the observed frequencies of various topologies.

The production of gamma rays and of neutral strange particles in these interactions has also been studied, by analysing electron pairs and V° decays observed in the bubble chamber (References 207 and 208). Table III shows the numbers of $\gamma$'s and $\pi^\circ$'s as functions of the number of charged particles produced, while Figure 1 shows the cross sections for the production of $K^\circ_s$, $\Lambda$ and $\bar{\Lambda}$ as a function of charged prong multiplicity.

---

4. A. Wroblewski, Acta Phys. Pol. B4, 857 (1973).

5. W. Busza et al., Phys. Rev. Letters 34, 836 (1975).

# Cross Sections for Production of Neutral Strange Particles

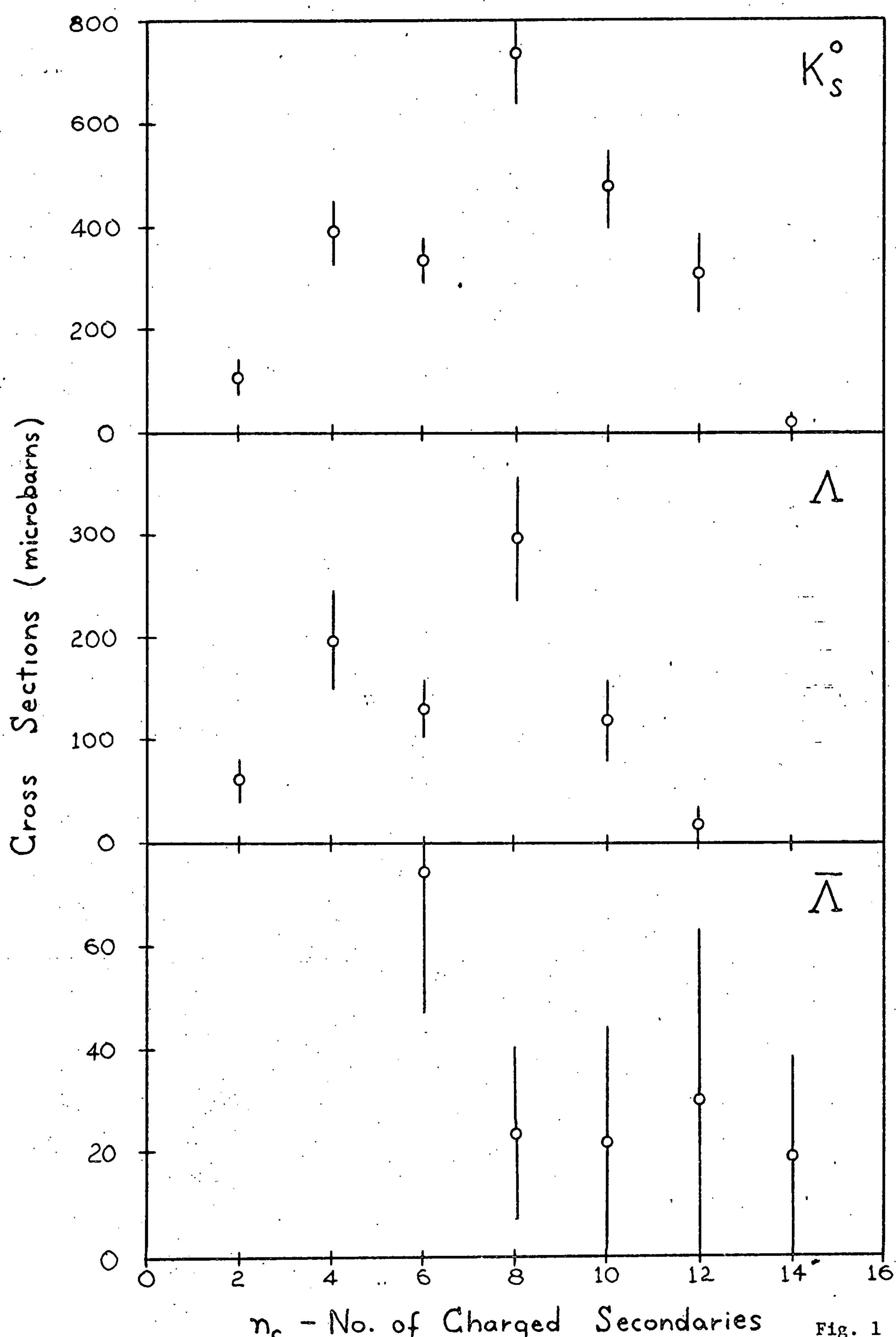


Fig. 1

These data are being refined, and in turn will be used to redetermine corrections to the charged prong numbers for unidentified Dalitz electrons, and for close electron pairs and close V° decays having vertices not distinguishable from the primary vertex.

(ii) Single Particle Momentum Distributions.

Inclusive production of various particles in reactions of the type $a + b \to c + X$, where c is the particle of interest and X is anything, has been of considerable interest for some time. The single particle distributions in the Feynman variable $x = 2p_L^*/\sqrt{s}$ and the rapidity $y = 1/2\ \ln((E^* + p_L^*)/(E^* - p_L^*))$, where $p_L^*$ is the longitudinal momentum and $E^*$ is the energy of particle c in the cm system, and $\sqrt{s}$ is the total invariant energy in the interaction, have been the subject of various model predictions. Figures 2 and 3 show the invariant cross sections in x for $\pi^- p \to \pi^- X$, and $\pi^- p \to \pi^+ X$, respectively. The experimental points are from this experiment, while the solid curve represents the data of the Aachen-Berlin-Bonn-Cracow-Heidelberg-Warsaw Collaboration at an incident momentum of 16.2 GeV/c. The similarity in these data is astonishing, and indicates that overall scaling is approached at momenta as low as 16 GeV/c, even for a particle combination ($ab\bar{c}$) with non-exotic quantum numbers. Our earlier experiment at 4.1 GeV/c indicated that scaling was approached in the target and projectile fragmentation regions even at that low momentum for $\pi^+ p \to \pi^- X$ ($ab\bar{c}$ exotic), in accordance with the ideas of Chan et al.,[6] but not for $\pi^+ p \to \pi^+ X$ ($ab\bar{c}$ non-exotic). The "Nova" model[7] predicts a shift and deepening of

---

6. H. M. Chan et al., Phys. Rev. Letters 26, 672 (1971).

7. M. Jacob and R. Slansky, Phys. Rev. D5, 1847 (1972).

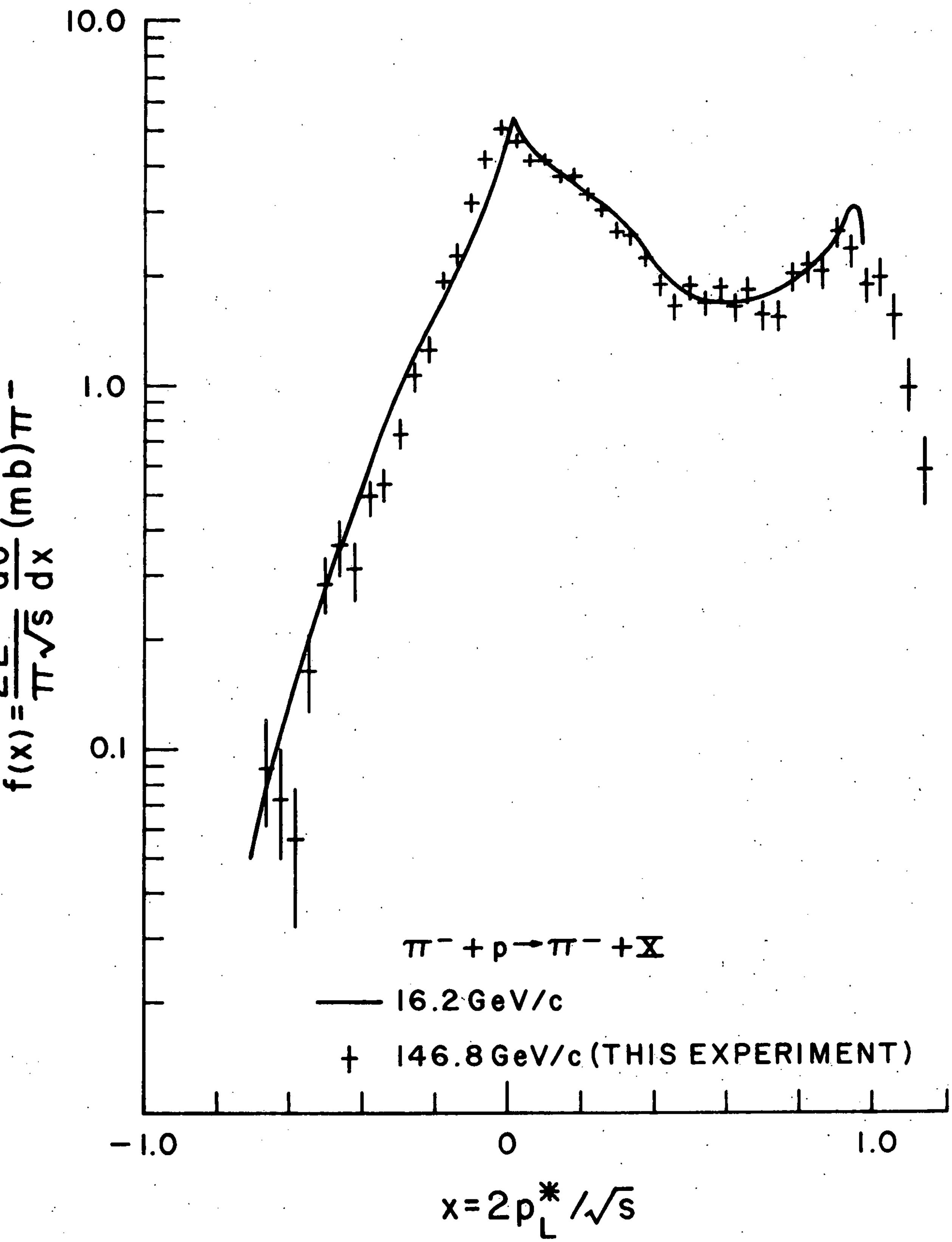

10.0
1.0
0.1
$f(x) = \frac{2E^*}{\pi\sqrt{s}} \frac{d\sigma}{dx}$ (mb) $\pi^-$
$\pi^- + p \rightarrow \pi^- + X$
16.2 GeV/c
146.8 GeV/c (THIS EXPERIMENT)
−1.0
0
1.0
$x = 2p_L^* / \sqrt{s}$


Figure 2

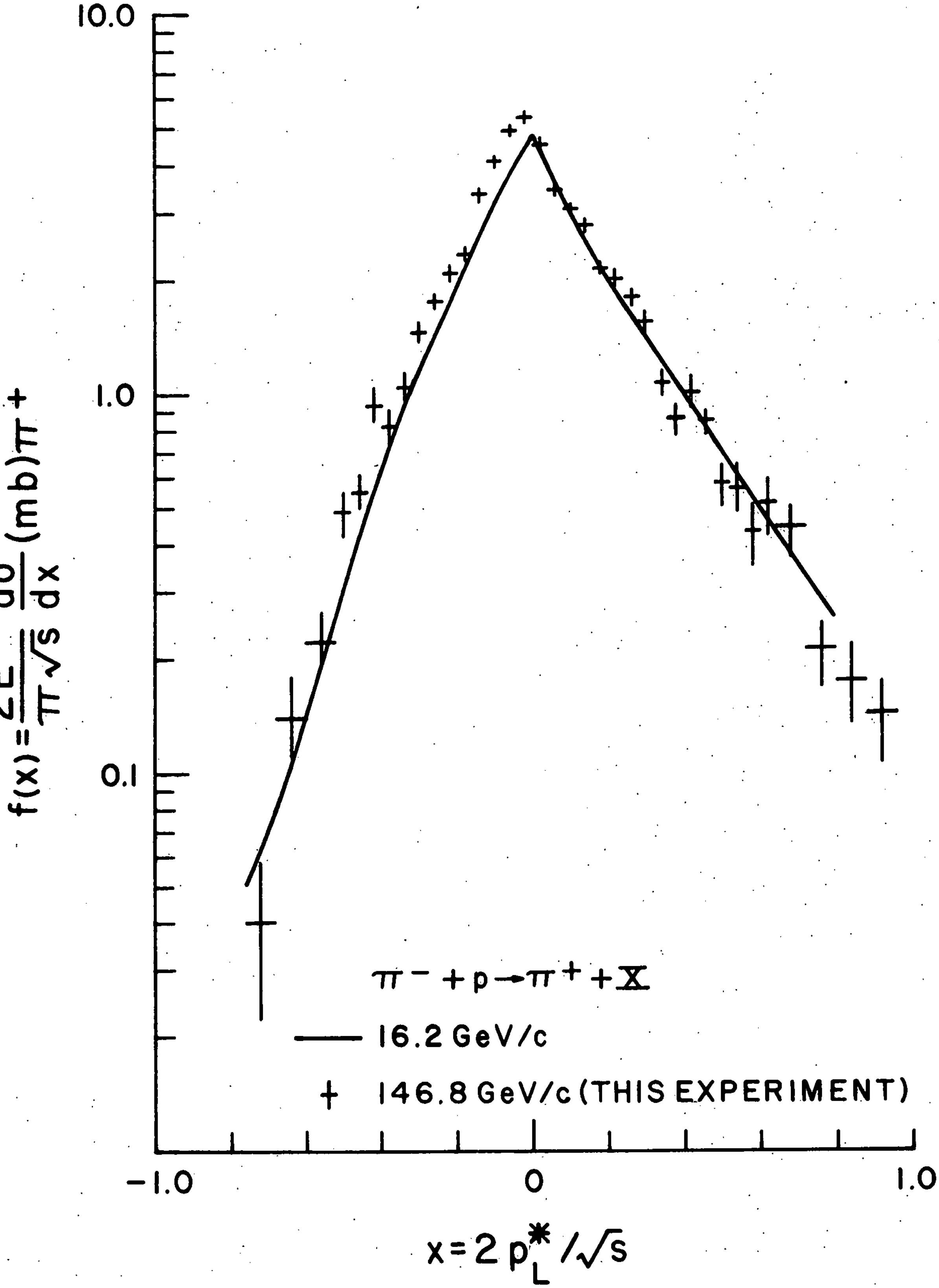
10.0
1.0
0.1
$f(x)=\frac{2E^*}{\pi\sqrt{s}}\frac{d\sigma}{dx}(mb)\pi^+$
$\pi^- + p \rightarrow \pi^+ + X$
16.2 GeV/c
146.8 GeV/c (THIS EXPERIMENT)
−1.0
0
1.0
$x = 2p_L^*/\sqrt{s}$

Figure 3

the dip in Figure 2 at FNAL energies, which appears to be contradicted by our data.

The distributions in rapidity for $\pi^- p \to \pi^- X$ and $\pi^- p \to \pi^+ X$ are shown in Figures 4 and 5, respectively, for both 16.2 GeV/c and 147 GeV/c $\pi^-$ beam momenta. In these two Figures, $d\sigma/dy$ is plotted, not the invariant cross section, and thus the 147 GeV/c data are considerably above the 16.2 GeV/c data. It is apparent, especially in Figure 5, that the distribution at the higher energy is much more asymmetric about the $y = 0$ axis than the lower energy distribution.

Mueller-Regge models[8] predict a $1/\sqrt{s}$ dependence in the value of $d\sigma/dy$ at $y = 0$ in the lab, and also predict that $\pi p$ and pp reactions will behave similarly if factorization is valid. Figure 6 shows $d\sigma/dy|_{y_{1ab} = 0}$ as a function of $1/\sqrt{s}$ , for $\pi^+$ and $\pi^-$ produced inclusively in $\pi^- p$, $\pi^+ p$ and pp interactions. The $\pi^+$ production points lie in an upper band, the $\pi^-$ in a lower band of the plot. Within each band, the points corresponding to exotic channels -- $pp \to \pi^+ X$, $pp \to \pi^- X$, $\pi^+ p \to \pi^- X$ -- have a smaller slope than those from non-exotic channels -- $\pi^+ p \to \pi^+ X$, $\pi^- p \to \pi^- X$, $\pi^- p \to \pi^+ X$. Within the uncertainties of the data, they are consistent with a $1/\sqrt{s}$ dependence; the major differences among the interactions arise not from the nature of the incoming particle but correspond to the charge of the outgoing particle and the exotic or non-exotic nature of the combination $ab\bar{c}$.

---

8. A. H. Mueller, Phys. Rev. D2, 2963 (1970); H. Boggild and T. Ferbel, Annual Reviews of Nuclear Science 24, 451 (1974) and references contained therein.

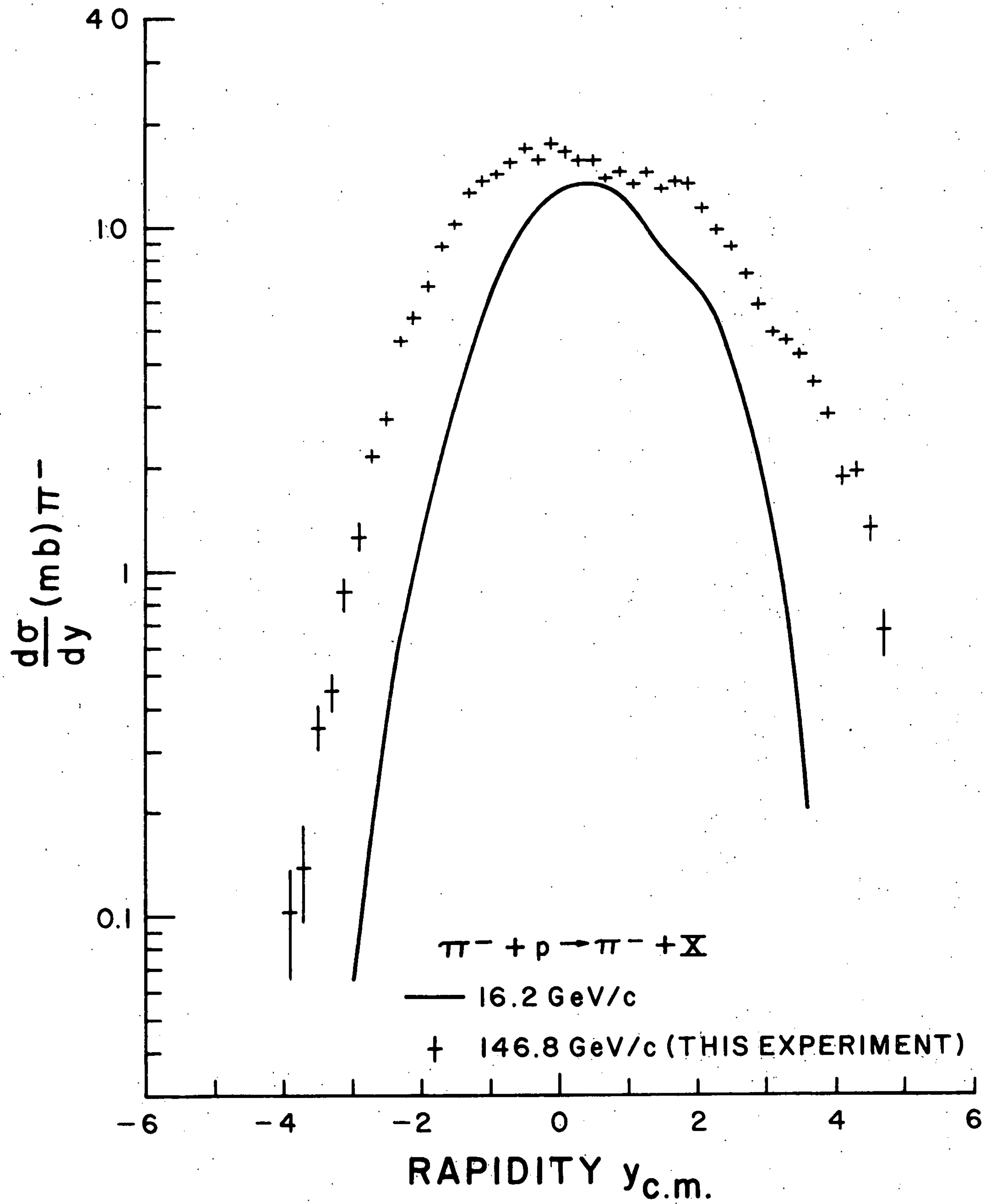

40
1.0
1
0.1
$\frac{d\sigma}{dy}$ (mb) π⁻
π⁻ + p → π⁻ + X
16.2 GeV/c
146.8 GeV/c (THIS EXPERIMENT)
-6
-4
-2
0
2
4
6
RAPIDITY $y_{c.m.}$


Figure 4

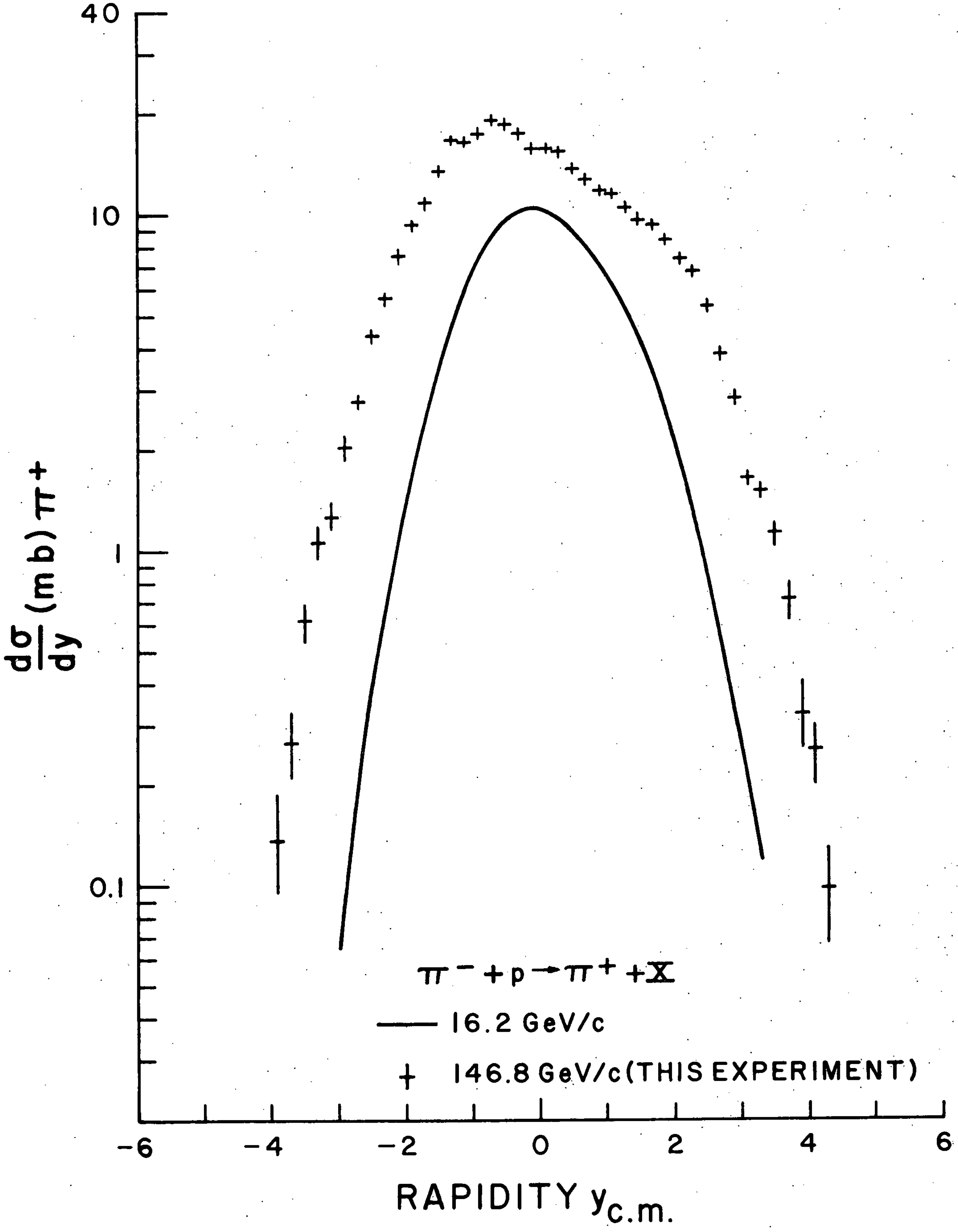

40
10
1
0.1
$\frac{d\sigma}{dy}$ (mb) $\pi^+$
$\pi^- + p \rightarrow \pi^+ + X$
16.2 GeV/c
146.8 GeV/c (THIS EXPERIMENT)
−6
−4
−2
0
2
4
6
RAPIDITY $y_{c.m.}$


Figure 5

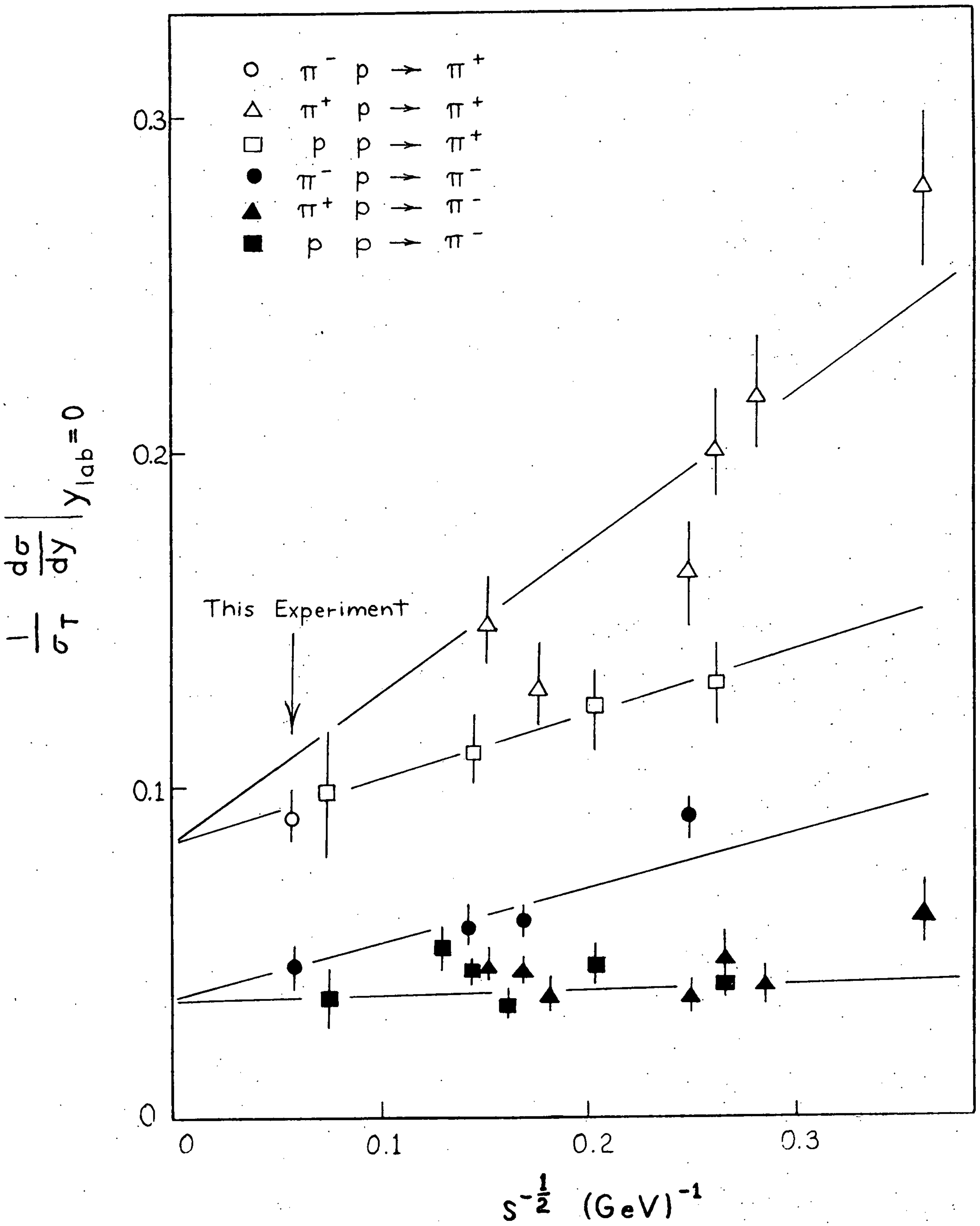

○ π⁻ p → π⁺
△ π⁺ p → π⁺
□ p p → π⁺
● π⁻ p → π⁻
▲ π⁺ p → π⁻
■ p p → π⁻
This Experiment
0.3
0.2
0.1
0
0.1
0.2
0.3
$\frac{1}{\sigma_T}\frac{d\sigma}{dy}\Big|_{y_{lab}=0}$
$s^{-\frac{1}{2}}$ (GeV)$^{-1}$


Figure 6

Figures 7 and 8 show distributions in x and y for the gamma rays in our experiment; these contrast with the corresponding plots for $\pi^- p \rightarrow \pi^- X$ and $\pi^+ X$ in that the distributions are contained in the central regions near $x = 0$ and $y = 0$ and away from the leading edges. (See Section C -- Reference 208).

Distributions in y have also been obtained for inclusive $\Delta^{++}$ (Figure 9) and $\rho°$ (Figure 10) production. The total cross sections are $1.55 \pm 0.19$ mb for $\pi^- p \rightarrow \Delta^{++} X$ and $6.38 \pm 1.78$ mb for $\pi^- p \rightarrow \rho° X$, with $\Gamma_\rho = 177$ MeV. The y distribution of $\Delta^{++}$ is heavily in the backward direction; for $\rho°$, with very poor statistics, the distribution peaks close to $y \approx 0.5 \pm 0.5$, while the y distribution for all $\pi^+\pi^-$ pairs has a broad peak centered at zero and is very close to symmetrical, especially for $|y| < 1.5$ . (See Section C - Reference 205).

(iii) Leading Particle Effects.

The distribution in x shown in Figure 2 for the outgoing $\pi^-$ from $\pi^- p \rightarrow \pi^- X$ shows a strong indication of a leading particle effect near $x = 1$ . The PHS system enables us to examine this in detail, as a function of prong number. The downstream wire chambers provide momentum measurements of fast forward particles not analyzable in the bubble chamber, while the bubble chamber allows us to determine the total charged prong number and the momenta of slower tracks, including leading protons produced with x close to -1. The system also gives a clean separation, on an event by event basis, of elastic and inelastic two-prong events. In the analysis of the single particle distributions, all negative

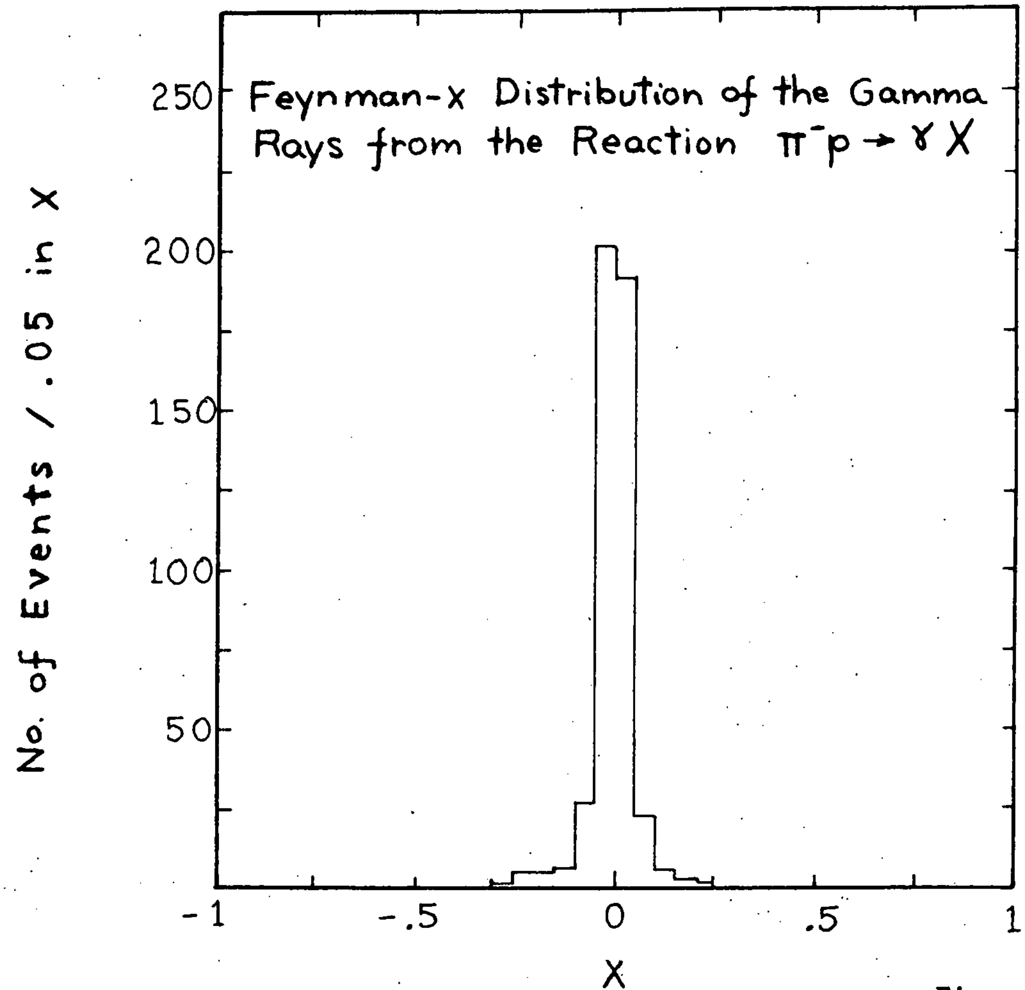


Figure 7

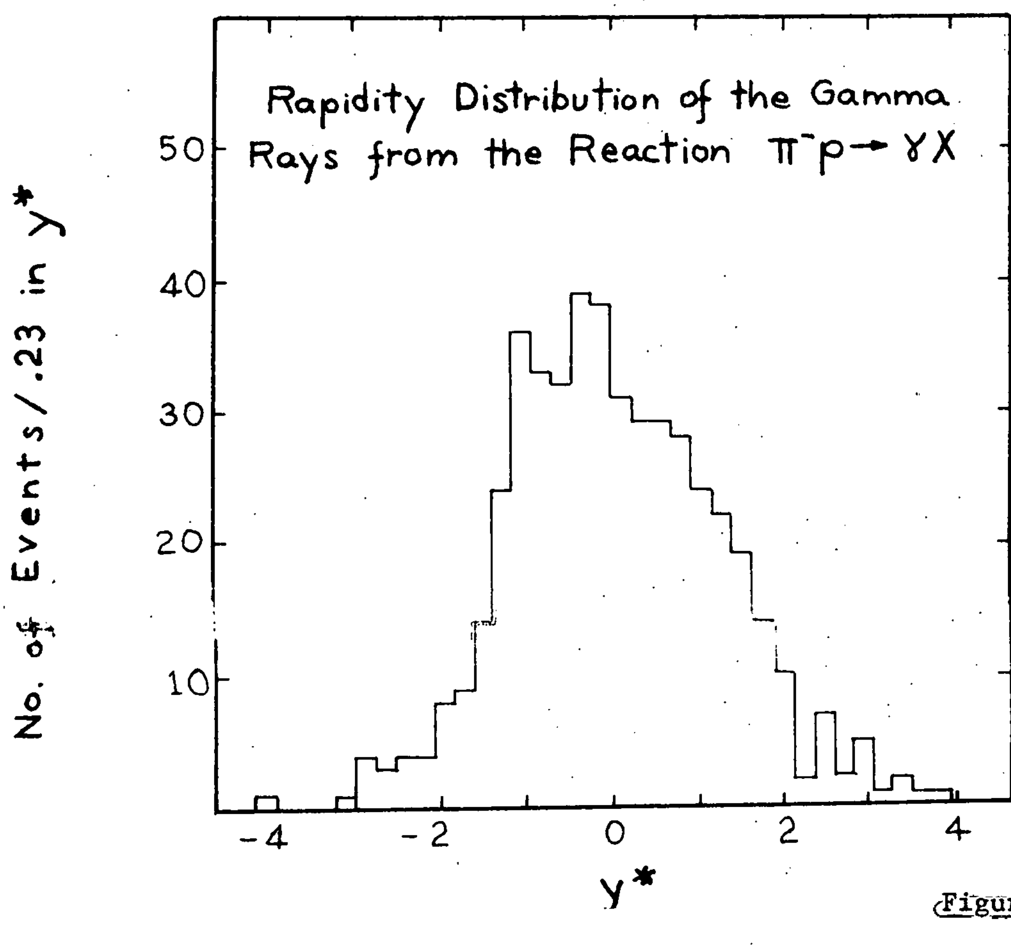


Figure 8

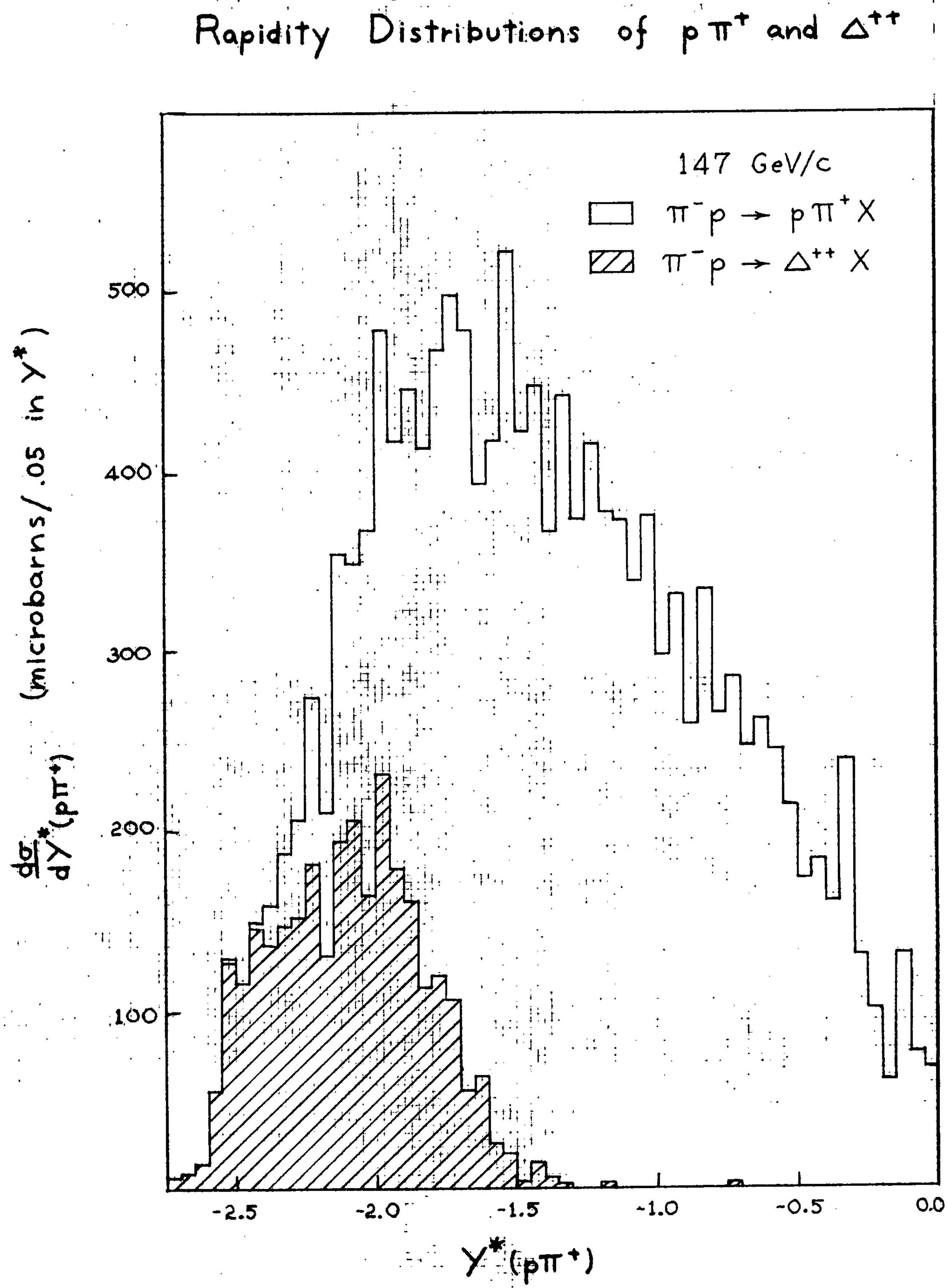
Rapidity Distributions of $p\pi^+$ and $\Delta^{++}$
147 GeV/c
$\pi^- p \to p\pi^+ X$
$\pi^- p \to \Delta^{++} X$
$\frac{d\sigma}{dY^*(p\pi^+)}$ (microbarns/.05 in $Y^*$)
500
400
300
200
100
-2.5
-2.0
-1.5
-1.0
-0.5
0.0
$Y^*(p\pi^+)$

Figure 9

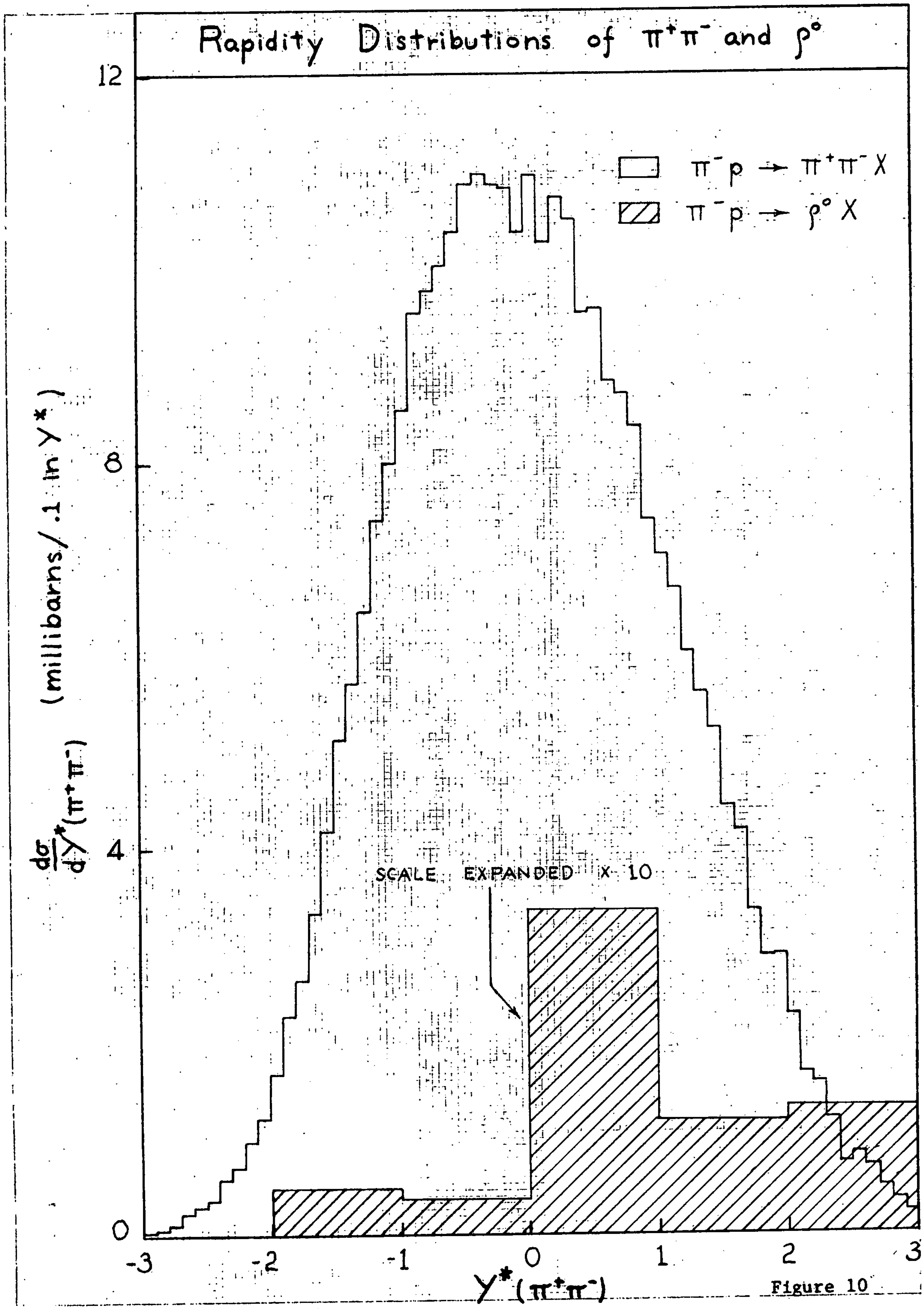

Rapidity Distributions of π⁺π⁻ and ρ°
12
8
4
0
$\frac{d\sigma}{dY^*}(\pi^+\pi^-)$ (millibarns / .1 in Y*)
π⁻p → π⁺π⁻X
π⁻p → ρ°X
SCALE EXPANDED X 10
-3
-2
-1
0
1
2
3
Y*(π⁺π⁻)


Figure 10

particles are assumed to be $\pi^-$, all positive particles not identified as protons on the basis of their ionization are assumed to be $\pi^+$.

We find that the leading particle peak is limited to events of low multiplicity. Figure 11 shows $d\sigma/dx$ vs. x for $\pi^-$ and $\pi^+$ mesons from inelastic events with two, four and six charged prongs; Figure 12 shows similar distributions for identified protons. The leading peak for $\pi^-$, very strong in two-prong events, diminished but still evident as a peak in four-prong events, has died to a low level in six-prong events, though particles with x close to 1 are still being produced.

In the proton x distribution, a leading particle peak is seen near x = -1 for two-, four- and six-prong events. In events with eight or more prongs, no leading peak is seen. Figure 13 shows the cross sections for leading particle production in two-, four- and six-prong events, compared with the total topological cross sections. Where the leading peak is well defined, the distributions in momentum transfer and in mass recoiling against the leading particles are indicative of diffraction scattering. However, whereas as much as 80% of the inelastic two-prong interaction cross section is consistent with low-mass diffraction excitation of the pion, proton or both, as described by a factorizable Pomeron exchange model, at least half the four- and six-prong final states are produced by some other mechanism (Reference 196).

(iv) Two-Prong Events.

Two techniques are used for separating elastic from inelastic two-prong events. As described in Reference 196, an accurate identification of elastic events is achieved by using the measured momentum in the

# Single Particle Feynman-x Distribution for $\pi^-$ and $\pi^+$

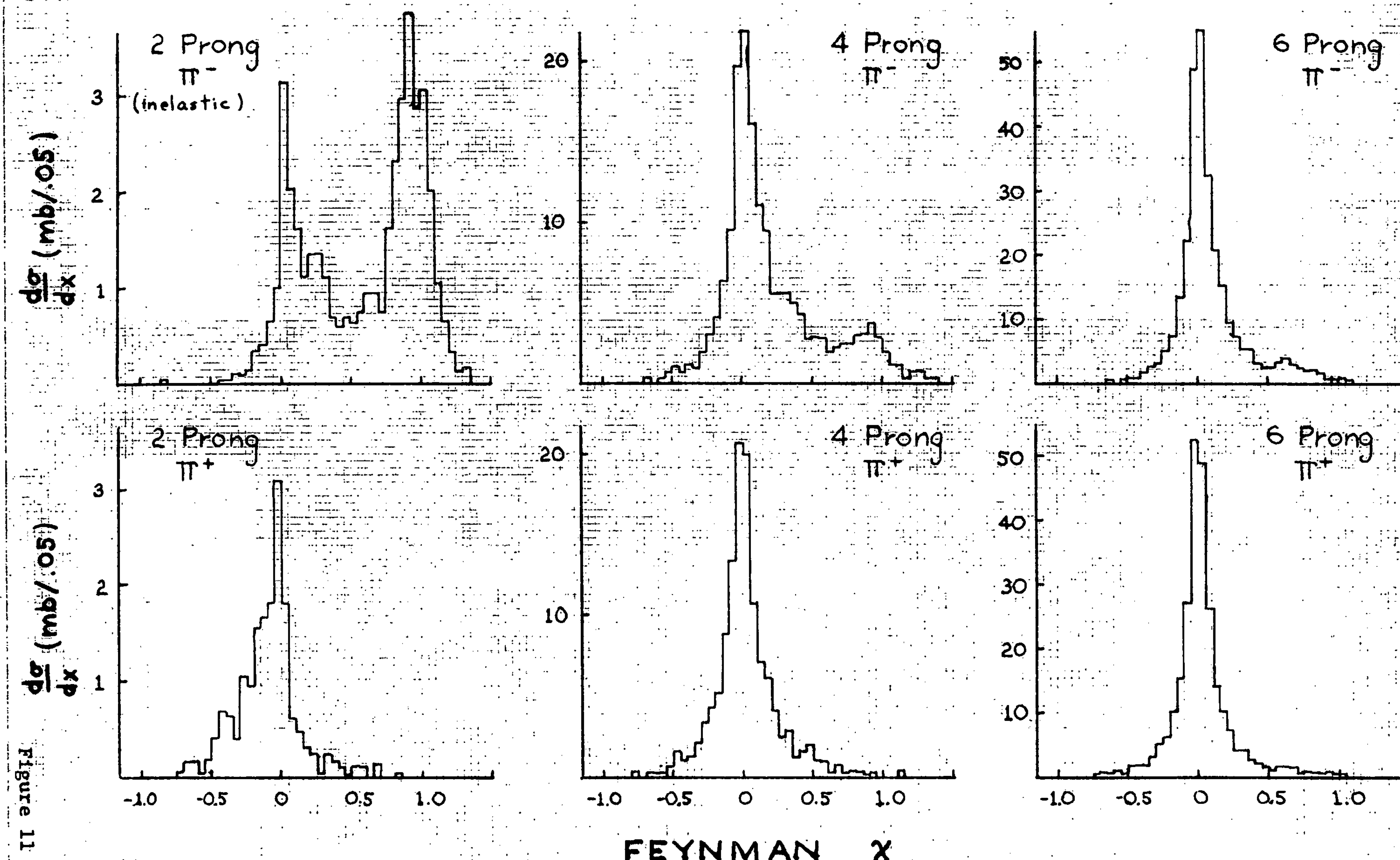


Figure 11

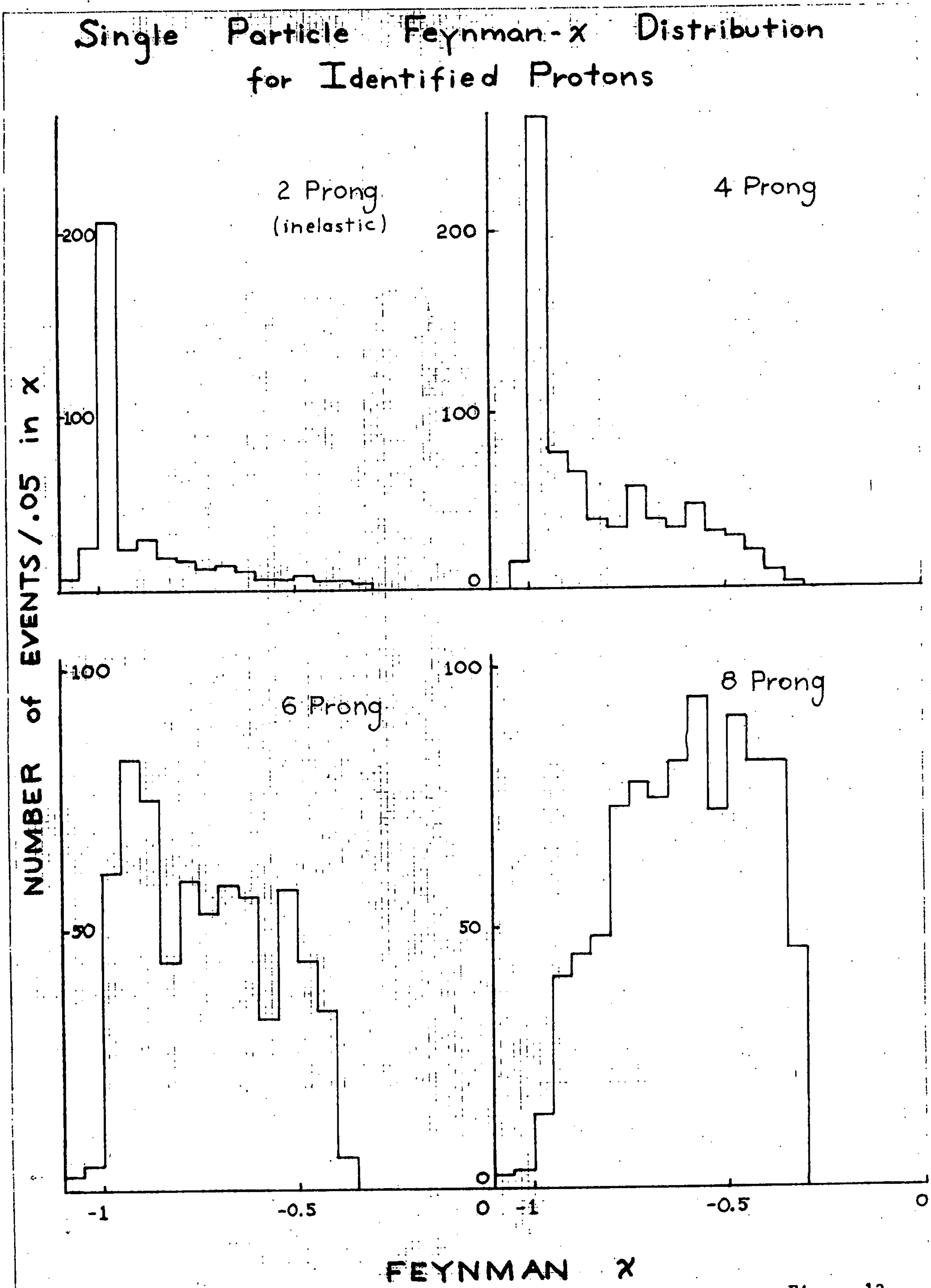
Single Particle Feynman-x Distribution
for Identified Protons
2 Prong
(inelastic)
4 Prong
6 Prong
8 Prong
NUMBER of EVENTS / .05 in x
FEYNMAN x
200
100
0
50
-1
-0.5

Figure 12

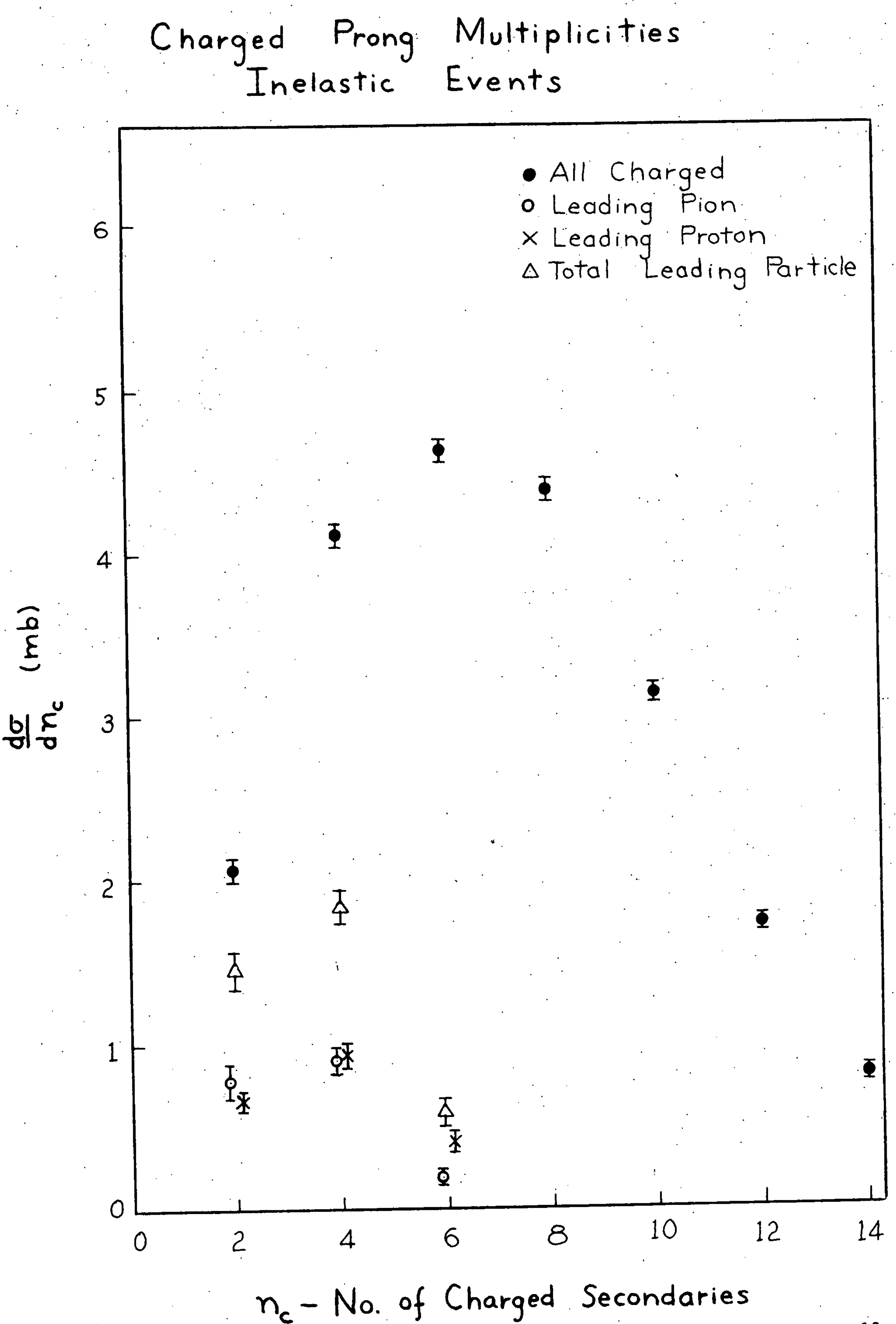

Charged Prong Multiplicities
Inelastic Events
All Charged
Leading Pion
Leading Proton
Total Leading Particle
$\frac{d\sigma}{dn_c}$ (mb)
0
1
2
3
4
5
6
0
2
4
6
8
10
12
14
$n_c$ – No. of Charged Secondaries


Figure 13

bubble chamber of the slow recoil proton to predict the path of the $\pi^-$ in the downstream chambers. For an event to be identified as elastic, the predicted and observed trajectories must agree, the spatial resolution in the downstream chambers being 0.5 mm and the angular resolution 0.1 mr. The second method is to use the kinematic fitting program SQUAW to determine the four-constraint fits. The results of the two procedures were found to be in excellent agreement. On the basis of studies of the events and Monte Carlo investigations, we estimate an upper limit of 5% elastic events wrongly classified as inelastic, with a similar number of inelastic events contaminating the elastic sample.

1. Elastic Scattering.

The cross section for elastic scattering is given in Table I. The differential cross section $d\sigma/dt$ is shown in Figure 14. It is quite well fitted over the range $0.04 \lesssim |t| \lesssim 0.4$ $(\mathrm{GeV}/c)^2$ by a single exponential of the form $Ae^{-bt}$, with $b = 8.6 \pm 0.5$ $(\mathrm{GeV}/c)^{-2}$. The apparent dip at low t is accounted for by systematic scanning losses of events with short recoil tracks.

2. Inelastic Two-Prong Interactions.

Inelastic two-prong events are divided between the following reactions, with the cross sections shown:

$$\pi^- + p \rightarrow \pi^- + p \quad + \text{neutrals} \qquad 1.31 \pm 0.15 \text{ mb} \qquad (1)$$

$$\pi^- + p \rightarrow \pi^- + \pi^+ \quad + \text{neutrals} \qquad 0.76 \pm 0.08 \text{ mb} \qquad (2)$$

Events of reaction (1), with $x_p < -0.95$, have a distribution in momentum tranfer from target to outgoing proton very similar to the elastic distribution shown in Figure 14 . In this, as well as in the $p\pi^-$

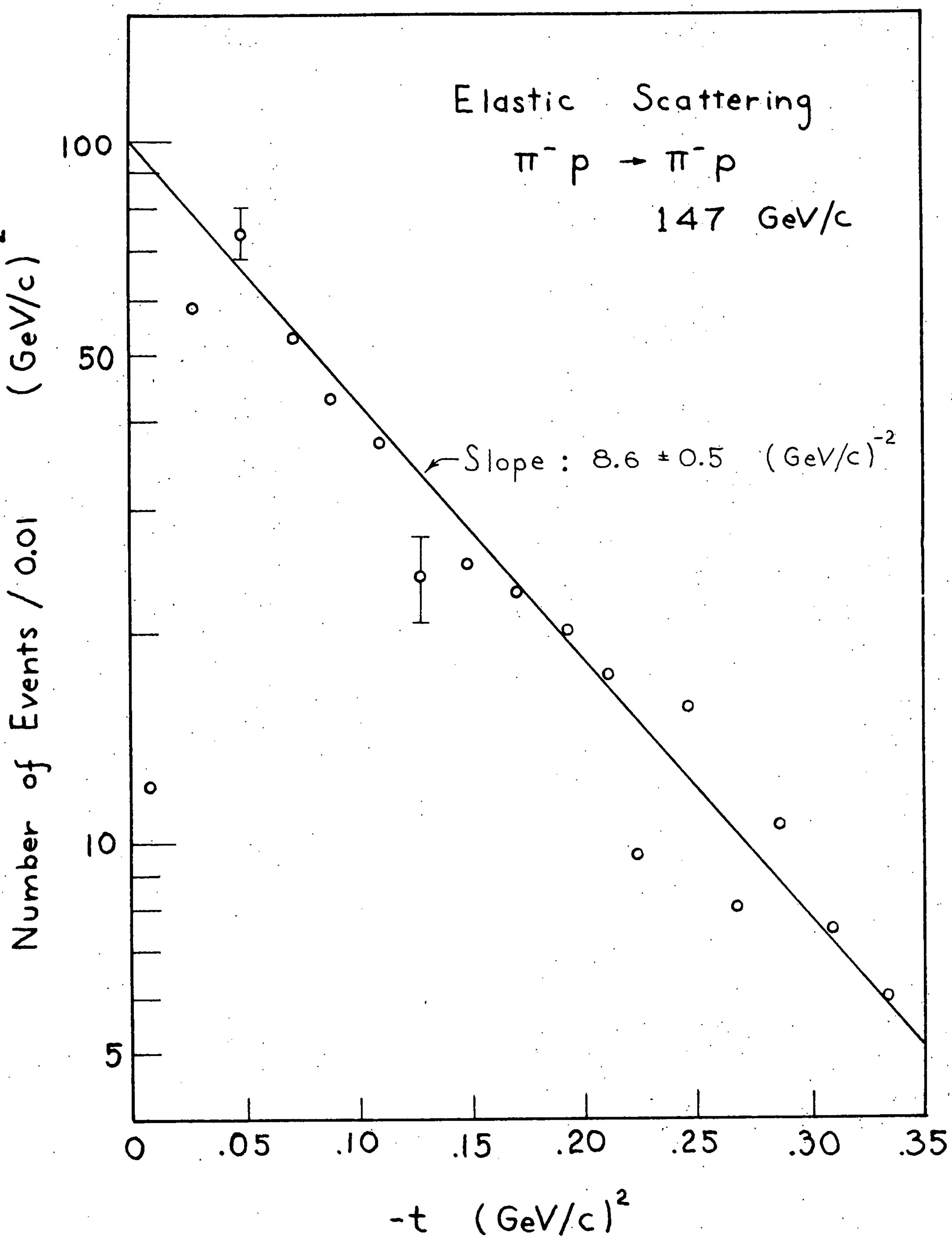

Elastic Scattering
$\pi^- p \rightarrow \pi^- p$
147 GeV/c
Slope : 8.6 ± 0.5 $(GeV/c)^{-2}$
Number of Events / 0.01 $(GeV/c)^{-2}$
100
50
10
5
0
.05
.10
.15
.20
.25
.30
.35
$-t$ $(GeV/c)^2$


Figure 14

invariant mass distribution and azimuthal correlation angle, they show the features characteristic of few-body diffractive excitation processes. These events are therefore assumed to be produced by diffractive excitation of the incident $\pi^-$, which can be represented by the diagram

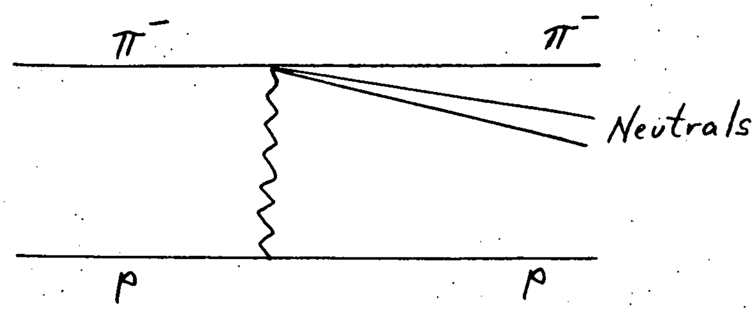


The cross section for this process in this experiment is found to be 780 ± 60 μb. Some of the events included here are "double leading", with $x_{\pi^-}$ close to +1. A mechanism of double Pomeron exchange[9] has been proposed for this:

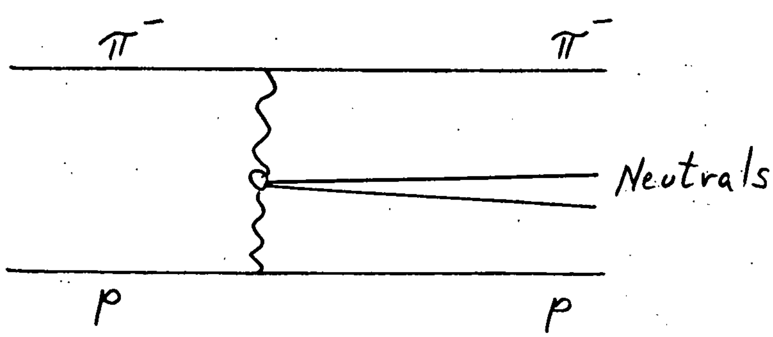


Our measured double-leading cross section is about one standard deviation higher than that predicted by this model (Reference 204). If the Pomeron singularity is a simple pole, these events should be isotropic in the

9. D. M. Chew and G. F. Chew, Physics Letters 53B, 191 (1974).

azimuthal angle $\phi$ between the transverse momenta of the leading $\pi^-$ and the leading proton. Instead they are peaked backward (i.e., $\phi$ between 90° and 180°), just as the other leading proton events are.

Target excitation is identified by $x_{\pi^-} > 0.76$, in both reactions (1) and (2), with $x_p > -0.95$ (that is, a non-leading proton) in reaction (1). The cross sections for excitation of the proton are found to be 350 ± 45 μb in reaction (1), and 420 ± 42 μb in reaction (2). The diagrams for the two cases are

(1)

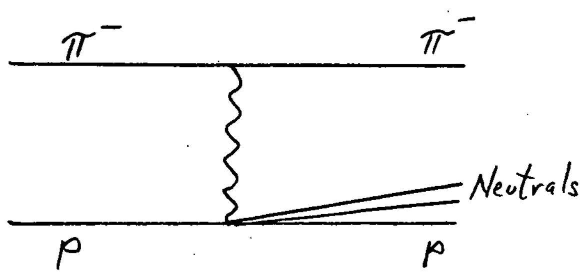


(2)

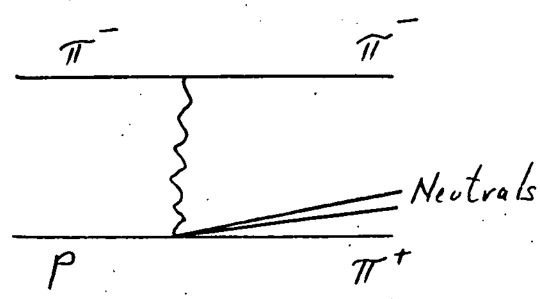


The beam and target diffraction discussed above account for about 75% of the inelastic cross section. The total diffractive contribution includes double diffractive processes illustrated by the diagrams

(1)

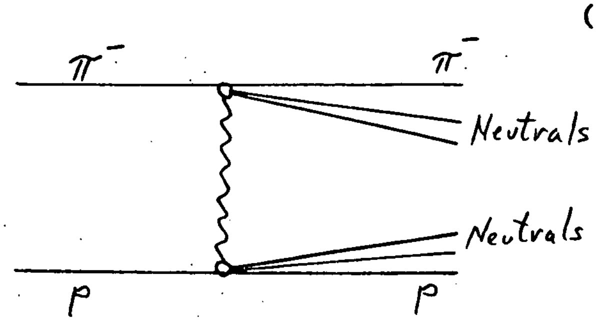


(2)

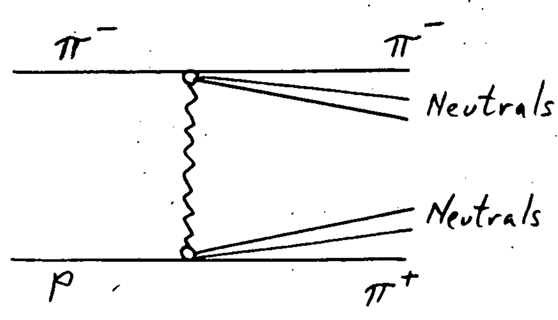


The cross sections for double diffraction excitation can be predicted from the single particle excitation cross sections if it is assumed that the particle exchanged is the Pomeron (as in elastic scattering) and that the amplitudes are factorizable into independent terms for each of the vertices. The results are 195 ± 24 μb for reaction (1) and 89 ± 17 μb for reaction (2), predicted from our measured single target and beam diffraction cross sections. The data are being studied to see if they are in agreement with these predictions.

A significant number of the $\pi^-$ mesons produced in reaction (2) have x values in the peak near x = 0. These cannot be accounted for by the diffractive processes discussed here. In these events, $x_{\pi+}$ is also close to zero. The effective mass distribution and the distribution in azimuthal correlation angle between the two charged mesons are characteristic of centrally produced pions in many-body final states. Probably the same mechanisms which dominate pion production in final states of higher charged multiplicities account for the non-diffractive component (∿15 percent) of the inelastic two-prong cross section.

(v) Other Subjects.

In addition to further detailed study of the subjects described in preceding sections, other investigations under way include the analysis of additional exclusive channels such as $\pi^- p \rightarrow \pi^- p \pi^+ \pi^-$, analysis of $\Delta^{++}$ and $\rho^\circ$ production, studies of particle correlations in multiprong events, and the topological cross sections for $K^-$ mesons which constitute about two percent of the negative particle beam.

In summary, the data of Experiment 154 are being explored by the

PHS Consortium in a multifaceted way, and are yielding a great deal of information on the nature of $\pi^-p$ interactions and on particle production mechanisms.

## II. Experimental Runs in Progress and in Preparation.

### a) A Study of $\pi^+p$, pp and $\pi^-p$ Interactions at 147 GeV/c in the Proportional Wire Chamber-Bubble Chamber Hybrid System (FNAL Experiment # 299).

This experiment by the Experiment #154 Consortium has been approved for 600,000 pictures, with a possible extension to $1.2 \times 10^6$ pictures, to be divided among $\pi^+$, p, and $\pi^-$ as beam particles, all at a momentum of 147 GeV/c. The purpose of this experiment is to study and to compare the characteristics of high energy interactions produced by the different projectile particles.

The first 158,000 frames of this experiment were obtained in a run of several weeks in January-February 1975. Martin Heller, a graduate student in our group, worked at FNAL during the entire run and was one of the experimenters principally repsonsible for the quality of the exposure. The beam was of positive particles, divided approximately evenly between $\pi^+$mesons and protons. The linking of the electronic data with the tracks in the bubble chamber allows us to use the upstream Cerenkov signal to identify each interacting beam particle. The results of this exposure, together with the $\pi^-$ data from Experiment 154, will enable us to make comparisons among the three different beam particles at an early stage.

We have decide to investigate initially the interaction channels leading to two, four, and six charged particles in the final state. This will make it possible for us to examine the behavior both of diffractive processes, which we have found dominate the two- prong $\pi^-$ interactions, and non-diffractive processes which become increasingly important at higher multiplicities.

For Experiment 154 all automatic measuring was performed on the MIT PEPR system. For Experiment 299, PEPR's at Yale, Rutgers and Johns Hopkins and probably the DOLLY at the University of Illinois will also be used. Considerable time was spent this spring devising improved scanning, IPD'ing, and PEPR'ing procedures to ensure uniform high-quality output data from this film. Scanning and pre-digitizing are now proceeding, and PEPR measuring will soon begin.

Last September a considerable up-grading of the 30" B.C.-hybrid system was proposed by the Consortium to FNAL (see Section C - Reference 193). Because of the tightness of funds, it was decided to proceed with the up-grading in small steps. As part of the first step a 1.2 m x 1.2 m drift chamber will be installed to improve the acceptance of the downstream system for secondary charged particles and a lead-glass Cerenkov system will be installed for the precise measurement of forward-going gamma ray energies and directions.

Brown is contributing to this effort in part through the construction of a counter telescope system to test the lead-glass counters. The counter telescope will define a thin pencil of high-energy electrons for calibrating the $\gamma$ counters and determining their characteristics as a function of position across the face of the $\gamma$ detector. The telescope will be constructed at Brown this summer and will be used at FNAL in the fall.

Further details on this experiment are presented in the accompanying Renewal Proposal.

b) Studies of Characteristics of Interactions as a Function of Beam Particle Momentum and Quantum Numbers (FNAL Proposals #375, #376, #377, and #378).

Four proposals were submitted to FNAL in February 1975, for experiments on $\pi^- p$ interactions at 75 and 300 GeV/c momentum, and for $K^+$ and $K^-$ mesons at about 150 GeV/c momentum. The $K^\pm$ exposures are contingent on the development of enriched beams, and the first phase of each of the $K^\pm$ proposals is directed toward the development of such beams. In each of these proposals Brown is collaborating with MIT, Yale, and CERN, with various other groups joining individual experiments. Further details concerning the experimental objectives are given in the Renewal Proposal.

(c) A Study of the Properties of the Forward-Going Photon Energy in the Two-Charged-Prong Topology Created in 150 GeV/c $\pi^- p$ Interactions (FNAL Proposal # 393).

In the further analysis of the 2-prong inelastic events of Experiment 154 we have recently noticed some unusual structure in the lab momentum distribution of the outgoing pion. Particularly in the projectile fragmentation region, where the leading proton is identified and has a

Feynman x value $< -0.95$, $p_{lab}$ of the $\pi^-$ has significant peaks around 10, 40, and 110 GeV/c. This is shown in Figure 15.

These data might be explainable by a reaction of the type

$$\pi^- p \rightarrow \text{"}A^-\text{"} + p$$

$$\text{"}A^-\text{"} \rightarrow \text{"}\rho^-\text{"} + \pi^\circ \quad \text{or} \quad \text{"}\rho^\circ\text{"} + \pi^-$$

$$\text{"}\rho^-\text{"} \rightarrow \pi^- + \pi^\circ \qquad \text{"}\rho^\circ\text{"} \rightarrow 2\pi^\circ$$

However, the "A" and the "ρ" would have to have properties very different from any A or ρ presently known. This might be evidence for a new phenomenon or new particles.

In order to investigate this further, the #154 Consortium submitted a proposal to FNAL this May with the above title. The lead-glass gamma detector being built for Experiment 299 would be excellent to measure the forward-going photon energy in the reaction $\pi^- p \rightarrow \pi^- p$ + neutrals. This experiment is discussed further in the Renewal Proposal.

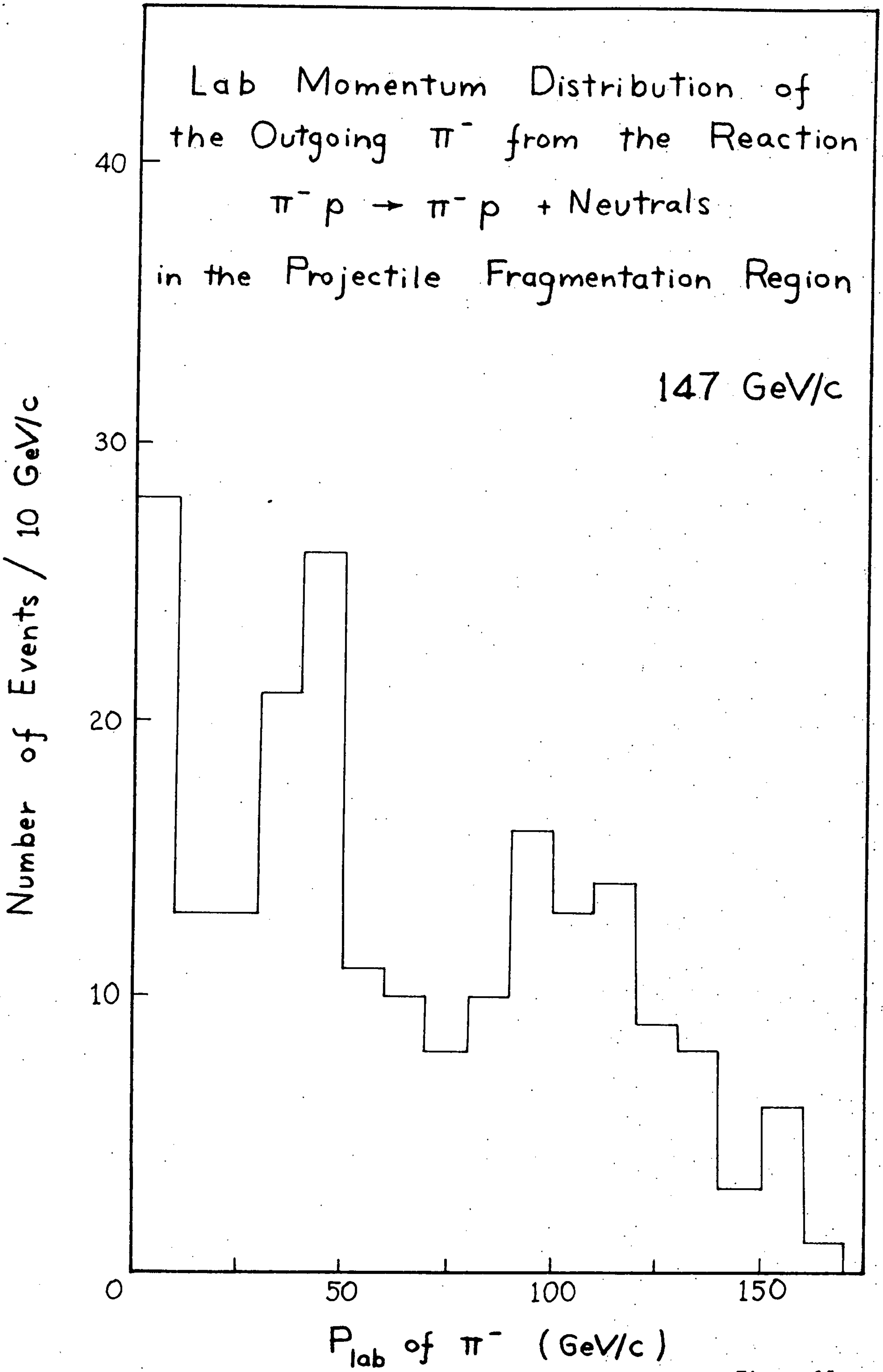
Lab Momentum Distribution of the Outgoing π⁻ from the Reaction
π⁻p → π⁻p + Neutrals
in the Projectile Fragmentation Region
147 GeV/c
Number of Events / 10 GeV/c
0
10
20
30
40
50
100
150
P lab of π⁻ (GeV/c)

Figure 15

## III. Associated Matters.

Professor Widgoff was elected this May to be a member of the Executive Committee of the User's Group at FNAL for a two-year term. She was also advanced from the position of Vice-Chairwoman last year to that of Chairwoman this year of the New England Section of the American Physical Society.

Professor Shapiro was invited to participate in the IV International Nucleon-Antinucleon Symposium at Syracuse University this May.

## IV. Scientific Personnel Associated with the Bubble Chamber-Proportional Hybrid System Program.

| | | |
|---|---|---|
| A. M. Shapiro | -- | Professor |
| M. Widgoff | -- | Professor |
| D. G. Fong | -- | Assistant Professor (Research) |
| A new Research Associate | | |
| M. Heller | -- | Graduate Research Assistant |
| A. Janos | -- | Graduate Research Assistant |

B. Electronic Detector and Spark Chamber Program.

I. Data Analysis in Progress.

a) Backward Pion Charge Exchange (AGS #416).

As was mentioned in our Renewal Proposal last year we expected to finish all work on this experiment by 1 January 1975. This has been the case. A paper, Ref. 210, summarizing the $\pi^- p \to n\pi^\circ$ results has been accepted for publication and another paper summarizing the $\pi^- p \to n\eta^\circ$ results is in preparation. We do not expect any further scanning, measuring or computing will be required on this experiment. We have not scanned and measured every energy available to us in our film; we believe that the essential physics has been extracted from the experiment and that finer energy steps than we have analysed by sampling energy values distributed over the whole range is not warranted presently.

As we have noted previously this is the first experiment in hadronic scattering where radiative corrections have been carried out. The corrections needed are as much as twelve percent at the highest energy and are nearly independent of invariant momentum transfer, u. The calculational methods needed to make these corrections for this experiment were reported in our Progress Report last year and are discussed in detail in Brown University High Energy Internal Report #131.

The corrected differential cross sections $d\sigma/du$ are shown in Fig. 1. The value of the momentum transfer u was calculated from the bisector of the c.m. opening angle for the two $\gamma$-ray events without a neutron measurement, and from an appropriately weighted average of the neutron and $\pi^\circ$(or single $\gamma$-ray) directions for the events with a detected neutron. The width of the data bins is typically more than twice the rms resolution, so that

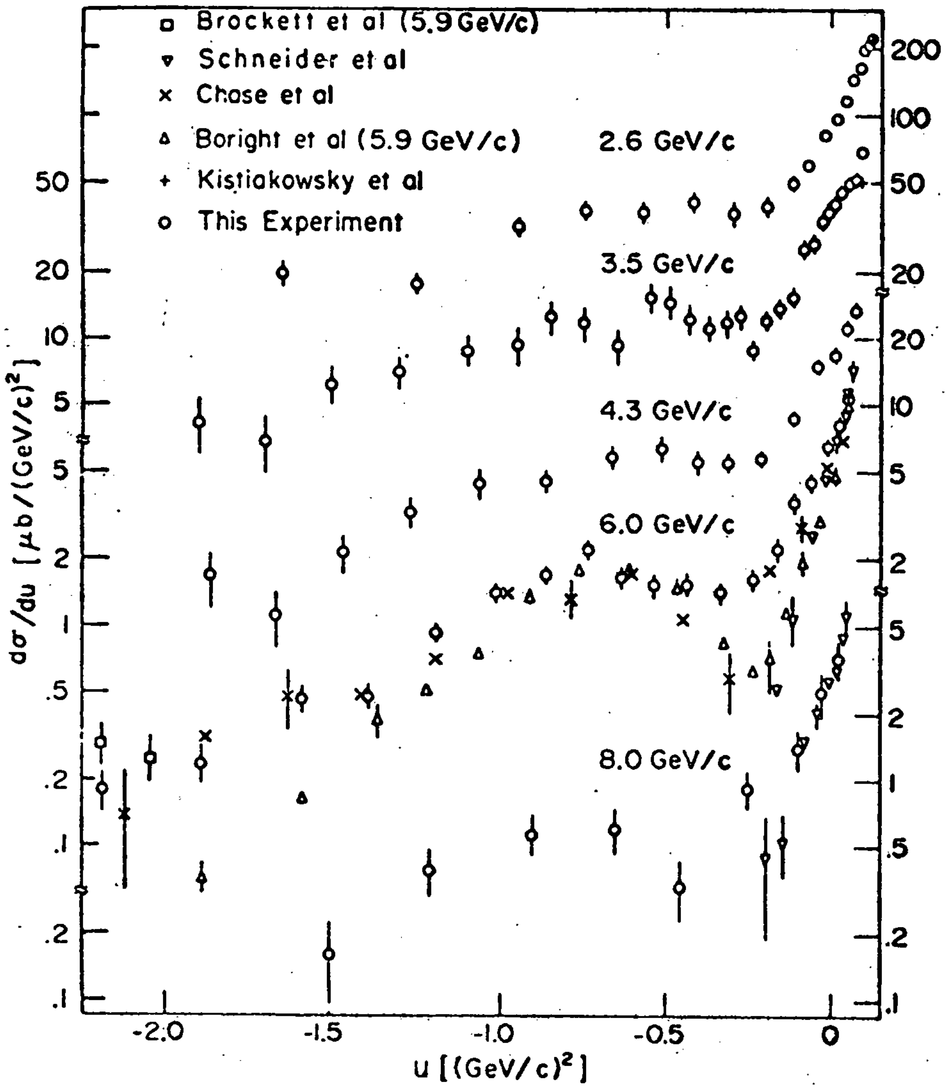


**Figure 1**

Differential cross sections for $\pi^- p \to n\pi^0$, including data from Ref. 2-6 with typical errors. The errors shown are statistical; normalization uncertainty is ~14%.

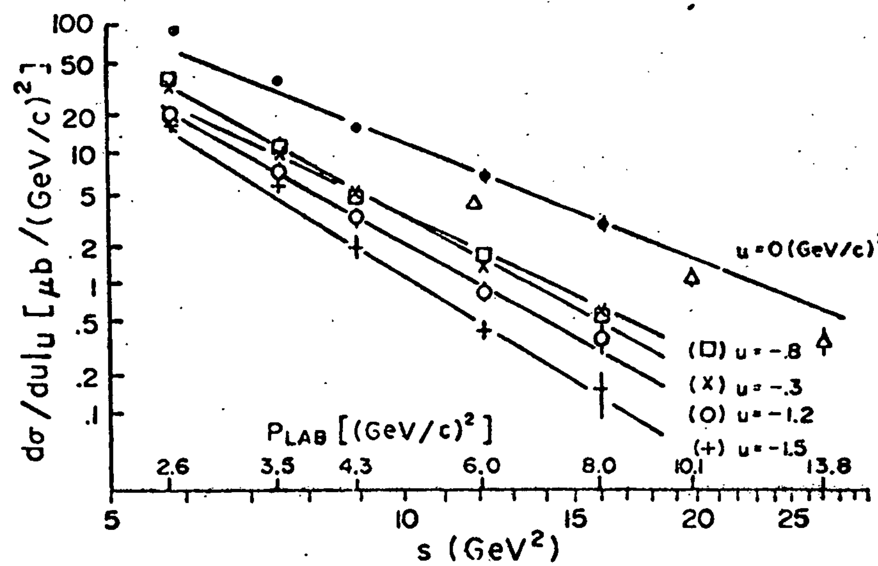


**Figure 2**

$d\sigma/du|_u$ vs. s at selected values of u. Lines are the results of fits to data at 4.3, 6.0, and 8.0 GeV/c with the form: $d\sigma/du \propto s^n$. Data from Ref. 3 (Δ) are included for u = 0.

resolution unfolding has produced only very slight changes from the experimental angular distributions. We have checked numerous experimental distributions which are sensitive to the resolution with Monte Carlo simulations with excellent results. Various other measures of u (e.g., only bisector, only neutron, etc.) yield angular distributions after resolution unfolding which are consistent, within statistical errors, with each other and with the results presented here.

The data all exhibit a backward peak, a shallow dip in the vicinity of $u = -0.3\ (GeV/c)^2$ and a shoulder or secondary maximum around $u = -0.7\ (GeV/c)^2$. The results of exponential fits to the data between $u_{max}$ and $u = -0.2\ (GeV/c)^2$ are given in Table 1.

We have included in Fig. 1 other angular distribution data at 6.0 and 8.0 GeV/c. It is clear that the data of Schneider et al.[2] and of Boright et al.[4] have steeper backward peaks than those of Chase et al.[3] and of this experiment. An exponential fit to the backward points of Ref. 3 gives a slope parameter $b = 6.4 \pm 1.1\ (GeV/c)^{-2}$ compared to $b = 11.3 \pm 1.2\ (GeV/c)^{-2}$ reported in Ref. 4. The experiments of Schneider et al. and Boright et al. both utilize only the two $\gamma$ rays in the analysis, whereas this experiment and Chase et al. have also detected and used the neutron direction with an improvement in momentum transfer resolution by almost a factor of three ($\Delta u \simeq .03$ for $u \simeq -.2$ at 6 GeV/c). Resolution unfolding cannot fully explain the discrepancy between the various measurements. The significantly smaller integrated backward cross section in the previous data (from 180° to the dip) might be due in part to sensitivity to Monte Carlo estimates of $\gamma$-ray losses. Our sample of one $\gamma$-ray events has made the largest fractional contribution just in this angular region (∿21% at 6 GeV/c). The trend of the data of Ref. 2 toward steeper peaks at lower energies could be explained by such sensitivity near $u = -0.1$ where their detection efficiency was only 5-10%. The data of Boright et al. also display a steeper falloff at large $|u|$ than the results of this experiment, of Chase et al., and of Brockett et al.[6]

Figure 1 also includes backward points measured by Kistiakowsky et al.[5] at 2.6, 3.5, and 6.0 GeV/c. Our data are in generally good agreement, but since none of the previous authors have applied radiative corrections appropriate for their experiments, comparisons principally of normalization may be misleading.

Table 1. Results of fitting data in backward peak ($-.2\ (\mathrm{GeV/c})^{-2} \lesssim u < u_{max}$) to form $d\sigma/du = a\, e^{bu}$

| $P_{lab}$ GeV/c | a $\mu b(\mathrm{GeV/c})^{-2}$ | b $(\mathrm{GeV/c})^{-2}$ |
|---|---|---|
| 2.6 | 93.8 ± 2.2 | 7.1 ± 0.3 |
| 3.5 | 37.6 ± 1.0 | 6.2 ± 0.4 |
| 4.3 | 17.4 ± 0.5 | 5.8 ± 0.4 |
| 6.0 | 7.2 ± 0.3 | 6.9 ± 0.6 |
| 8.0 | 3.1 ± 0.4 | 7.6 ± 2.3 |

In Fig. 2 we have plotted values of $d\sigma/du$ at various fixed values of u versus s on a logarithmic scale. The three higher energy points at each value of u have been fitted to a power law dependence, $As^n$. In terms of a simple Regge model where $n = 2\alpha(u)-2$ we obtain $\alpha(0) = -.48 \pm .06$ which is consistent with, but somewhat lower than, the intercept customarily accepted for the $N_\alpha$ trajectory, viz., $\alpha \approx -.4 + .9u$.

The dominance of the $N_\alpha$ trajectory in $\pi N$ backward scattering in the energy region 5-20 GeV has been advanced as an explanation of the deep dip observed in $\pi^+p$ scattering near u = -.15 at all energies above a few GeV.[8,9] In models of backward charge exchange both with an $N_\alpha$ nonsense wrong signature zero or with cuts, a dip occurs that should be only slightly shifted from that in $\pi^+p$.[1] Over the range of energies covered by this experiment the shallow dip seen in our data does not occur at the same values of u as for $\pi^+p$, nor does it approach the same value of $u' = u-u_{max}$.[10]


1 See for example: E. L. Berger and G. C. Fox, Nucl. Phys. B26, 1 (1971), and V. Barger and D. Cline, Phenomenological Theories of High Energy Scattering (Benjamin, New York, 1969).

2 J. Schneider et al., Phys. Rev. Lett. 23, 1068 (1969).

3 R. C. Chase et al., Phys. Rev. D2, 2588 (1970).

4 J. P. Boright et al., Phys. Lett. 33B, 615 (1970).

5 V. Kistiakowsky et al., Phys. Rev. D6, 1882 (1972).

6 W. S. Brockett et al., Phys. Lett. 51B, 390 (1974).

7 F. Bulos et al., Phys. Rev. 187, 1827 (1969).

8 C. B. Chiu and J. D. Stack, Phys. Rev. 153, 1575 (1967).

9 V. Barger et al., Nucl. Phys. B49, 206 (1972).

10 V. Barger et al., Nucl. Phys. B57, 401 (1973).

b) A $\bar{p}p \to$ Bosons (in the T and U-mass region) AGS Spark Chamber Experiment (AGS #527).

The physics of this experiment (and AGS #622, mentioned below) is primarily directed to searching for high mass, high spin bosons, however it is also very closely related to that of the backward scattering experiment just discussed in the previous section. Typical reactions are $\bar{p}p \to \pi^\circ\pi^\circ$, $\eta^\circ\eta^\circ$, $\pi^\circ\eta^\circ$, $\pi^\circ f^\circ$. The point of the experiment is to study the angular distributions of these reactions as a function of incident antiproton energy. The energy region involved permits the study of the mass range up to 2500 MeV. This range continues to be a very perplexing one in particle physics as there are persistent suggestions for at least eight mesons of as yet undetermined quantum numbers. The explicit nature of the quantum numbers in the final states mentioned above, together with an analysis of their angular distributions will permit unambiguous determination of the parameters for any of these heavy mesons. In addition, by crossing symmetry, these final states are closely related to backward meson scattering, the interchange of the roles of the s- and t-channel resonances and Regge trajectories in these processes presents an ideal situation in which to study the predictions of models involving "duality" such as the Veneziano model.

Running at the AGS for this experiment was completed in early January 1973. Approximately 750K total photographs were taken. These pictures being evenly divided for scanning and measuring amongst the collaborators -- Bari (Italy), Brown and MIT.

Our first scanning and measuring indicated we might expect angular distributions at the lower mass range containing roughly 500 events each in the channel $\bar{p}p \to \pi^\circ\pi^\circ$ with a mass resolution of 8 MeV or with higher statistics with somewhat coarser binning. The mass interval covered is continuous from 2080 MeV to 2580 MeV and since the cross section is falling as a power of s there are fewer events at the higher masses. Although no experiment has been done previously on $\pi^\circ\pi^\circ$ (or other neutral non-strange channels), this one has nearly a factor of 5 improvement over the mass resolution in a related $\bar{p}p \rightarrow \pi^+\pi^-$ experiment. In addition to $\pi^\circ\pi^\circ$, we have determined from our electronic rates that there are roughly 250 microbarns in other channels leading to two or more gamma rays in the final state. These could be from $\pi^\circ\eta^\circ, \pi^\circ\omega^\circ, \pi^\circ f^\circ$, $2\pi^\circ\omega^\circ$, as well as from simple phase space. This cross section corresponds to about ten times that in $\pi^\circ\pi^\circ$ and so, although more difficult to analyze, are expected to provide adequate angular distributions even with severe kinematic cuts. If resonances occur these data will provide branching ratios and additional isospin information.

We have pointed out previously the complete extraction of all of the physics which it is possible to study in this film is a formidable task because of the high gamma ray multiplicity and the large number of energy steps. Consequently, we adopted the strategy early in our analysis that we would concentrate first upon the reactions $\bar{p}p \rightarrow \pi^\circ\pi^\circ$, $\pi^\circ\eta^\circ$ and $\eta^\circ\eta^\circ$ which require measurement of multiplicities of 1 through 5 gamma rays. Also we decided to begin by an energy selection which "clumped" the energies but distributed the clumps over the full energy range. Proceeding in this way we have completed about one third of the data.

The last of the major components for the extensive computer programming system needed to carry out the four gamma (i.e., $\pi^\circ\pi^\circ$, $\eta^\circ\pi^\circ$, $\eta^\circ\eta^\circ$) analysis has been completed and we are moving into a situation which will hopefully be routine production. Computer emphasis will then shift to the rather more general problems of physics analysis.

The results from the first six energies were presented a few weeks ago at the IV International Symposium on Nucleon-Anti-nucleon Interactions held at Syracuse, N.Y. The results are interesting, surprising and elicited much interest. Results for the single energy, 1.752 GeV/c, were presented at the Nucleon-Anti-nucleon Symposium held in Prague last summer (see Ref. 211).

Summarizing briefly, the results so far are as follows:

1) The energy dependence of the partial cross section for both the $\bar{p}p \rightarrow \pi^\circ\pi^\circ$ and $\bar{p}p \rightarrow \pi^\circ\eta^\circ$ are in general smoothly falling, however both have suggestions of structure -- at 1.719 GeV/c in the former and at 1.752 GeV/c in the latter (see Figures 3 and 4). There is also the rather striking feature in the $\pi^\circ\pi^\circ$ case that it has a shape very similar to the $\bar{p}p \rightarrow \pi^+\pi^-$ data of Eisenhandler et al;[11] the $\pi^+\pi^-$ is a mixture of both I = 0 and I = 1 while the $\pi^\circ\pi^\circ$ is pure I = 0.

2) The absolute and relative sizes of the three partial cross sections are also surprising. All three cross sections were unmeasured previous to this experiment. First, it is found that the cross section to $\pi^\circ\pi^\circ$ would seem to be about one half that expected from crossing symmetry arguments. This will be a significant difficulty for simple exchange models.

For the $\pi^\circ\eta^\circ$ and $\eta^\circ\eta^\circ$ channels there is the totally unexpected result that they have cross section values in general larger than the $\pi^\circ\pi^\circ$ one and that their ratio to the $\pi^\circ\pi^\circ$ cross section is virtually independent of energy although again there could conceivably be structure. If exchange mechanisms are involved one might expect different energy dependences amongst them since different quantum numbers are exchanged. In Figure 5, we show the $\pi^\circ\eta^\circ$ to $\pi^\circ\pi^\circ$ ratio. The

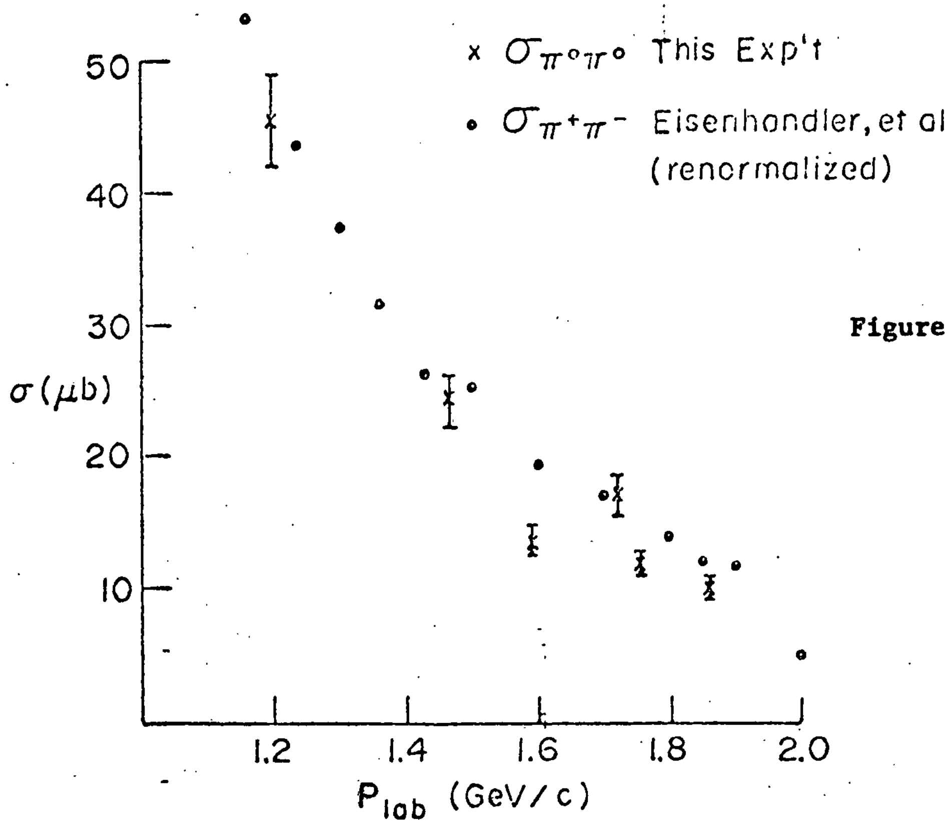


**Figure 3**

Total Cross Section $\bar{p}p \to \pi^0\eta^0$

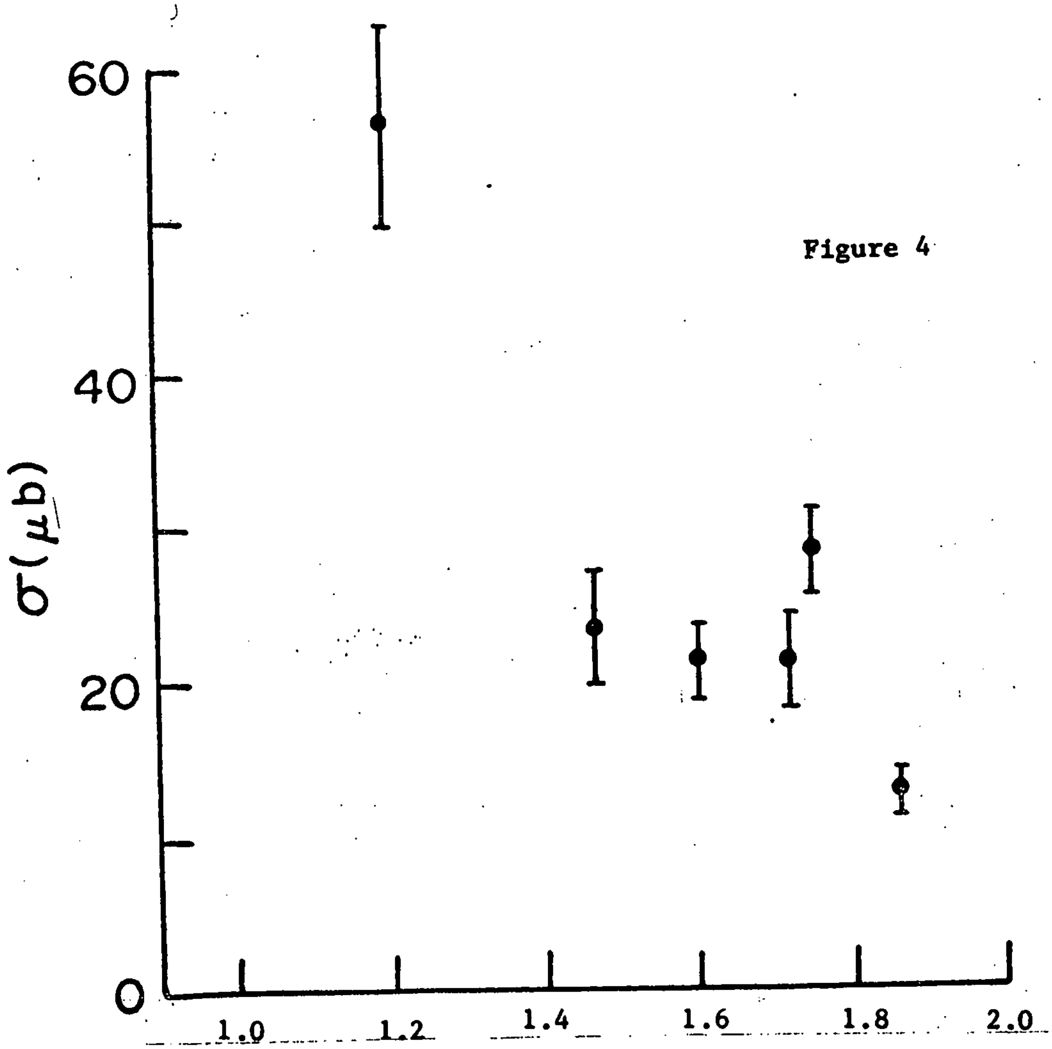


**Figure 4**

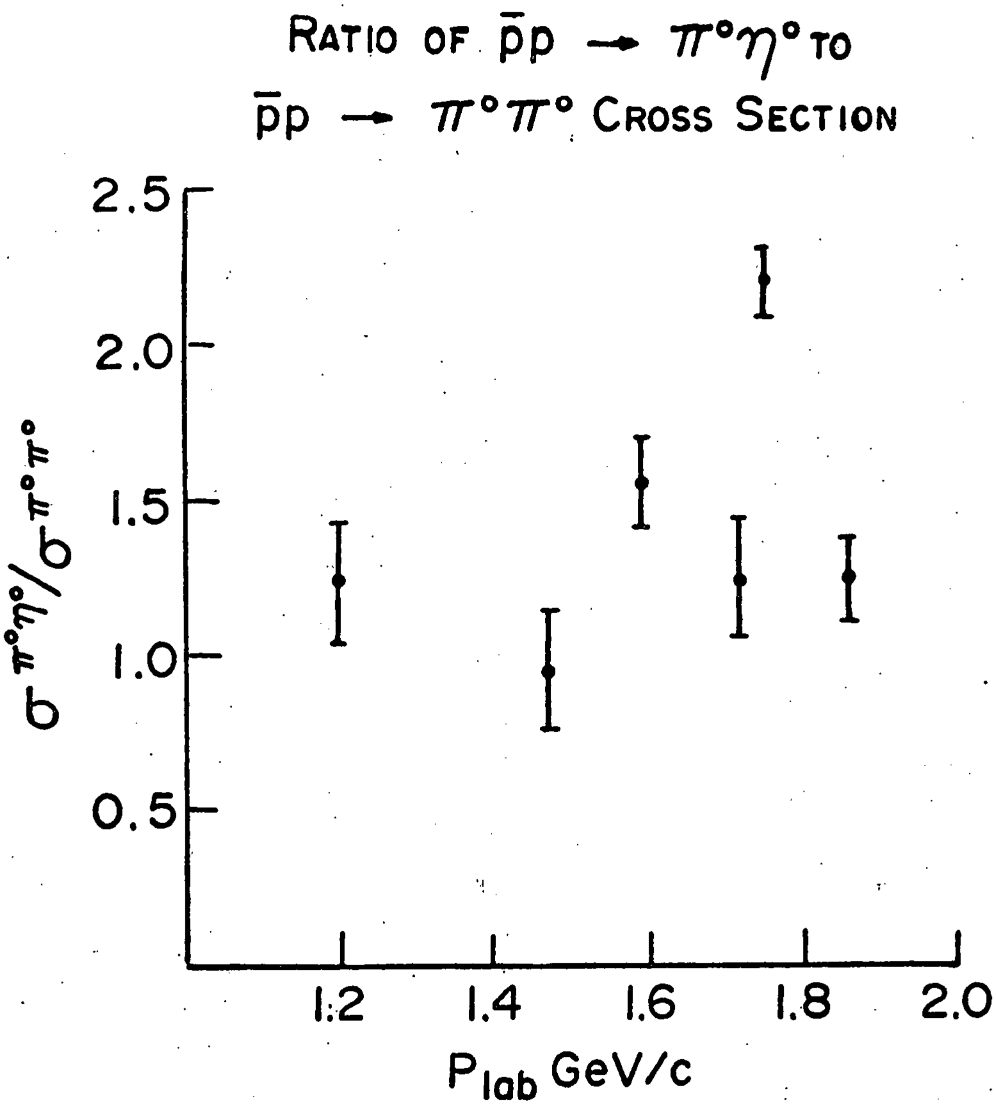

RATIO OF $\bar{p}p \rightarrow \pi^\circ\eta^\circ$ TO
$\bar{p}p \rightarrow \pi^\circ\pi^\circ$ CROSS SECTION
2.5
2.0
1.5
1.0
0.5
$\sigma^{\pi^\circ\eta^\circ}/\sigma^{\pi^\circ\pi^\circ}$
1.2
1.4
1.6
1.8
2.0
$P_{lab}$ GeV/c


Figure 5

$\eta^\circ\eta^\circ$ cross section is 10.3 ± 4.2μb at 1.752 GeV/c and 7.75μb ± 2.6μb at 1.862 GeV/c. These cross sections involving eta mesons which are large relative to those involving just $\pi^\circ\pi^\circ$'s may also have relevance to the so-called "energy crisis" suggested in the $e^+e^-$ annihilation experiments at SPEAR. In those experiments they find only 55% of the total energy in $e^+e^- \rightarrow$ HADRONS appears as charged particles. It is difficult to explain this in terms of missing $\pi^\circ$'s only.[12] If there were a significant number of $\eta^\circ$'s produced then it ceases to be a "crisis". The quantum numbers of the $\bar{p}p$ states are comparable to the $e^+e^-$ states and consequently there is a justifiable comparison.[13,14]

3) The angular distributions which we find are quite unexpected in their apparent "purity" of states considering the seemingly absent sharp energy dependence one would expect from narrow resonances -- the analysis of these angular distributions is potentially the most significant part of the experiment. In Figures 6 and 7 are shown the angular distributions we have found for $\pi^\circ\pi^\circ$ and $\eta^\circ\pi^\circ$, respectively. In Figures 8 and 9 are shown the Legendre polynomial coefficients which are extracted for these distributions. The features of these distributions are the progression of the dips and peaks from lowest to highest momentum, and the hard zeros at the dips which tend to indicate almost pure states.

Figure 8 also shows a comparison of the normalized Legendre coefficients for $\bar{p}p \rightarrow \pi^\circ\pi^\circ$ and $\bar{p}p \rightarrow \pi^+\pi^-$. To facilitate the comparison we have interpolated the coefficients of Eisenhandler et al.[11] to our nominal momenta. The general agreement is quite surprising since $\pi^+\pi^-$ is a mixture of I = 0 and I = 1.

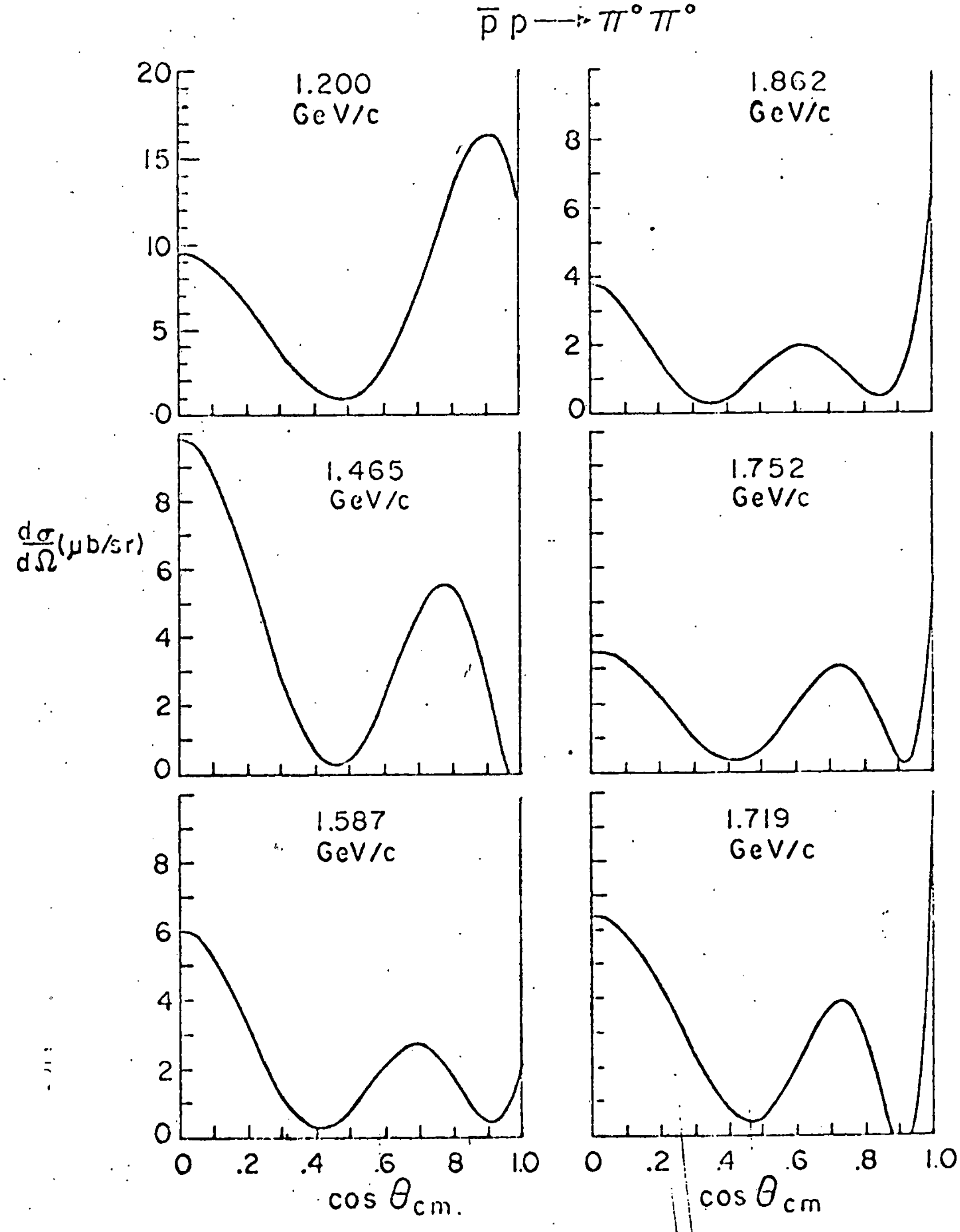


Figure 6 Fitted angular distributions $\bar{p}p \to \pi^0\pi^0$

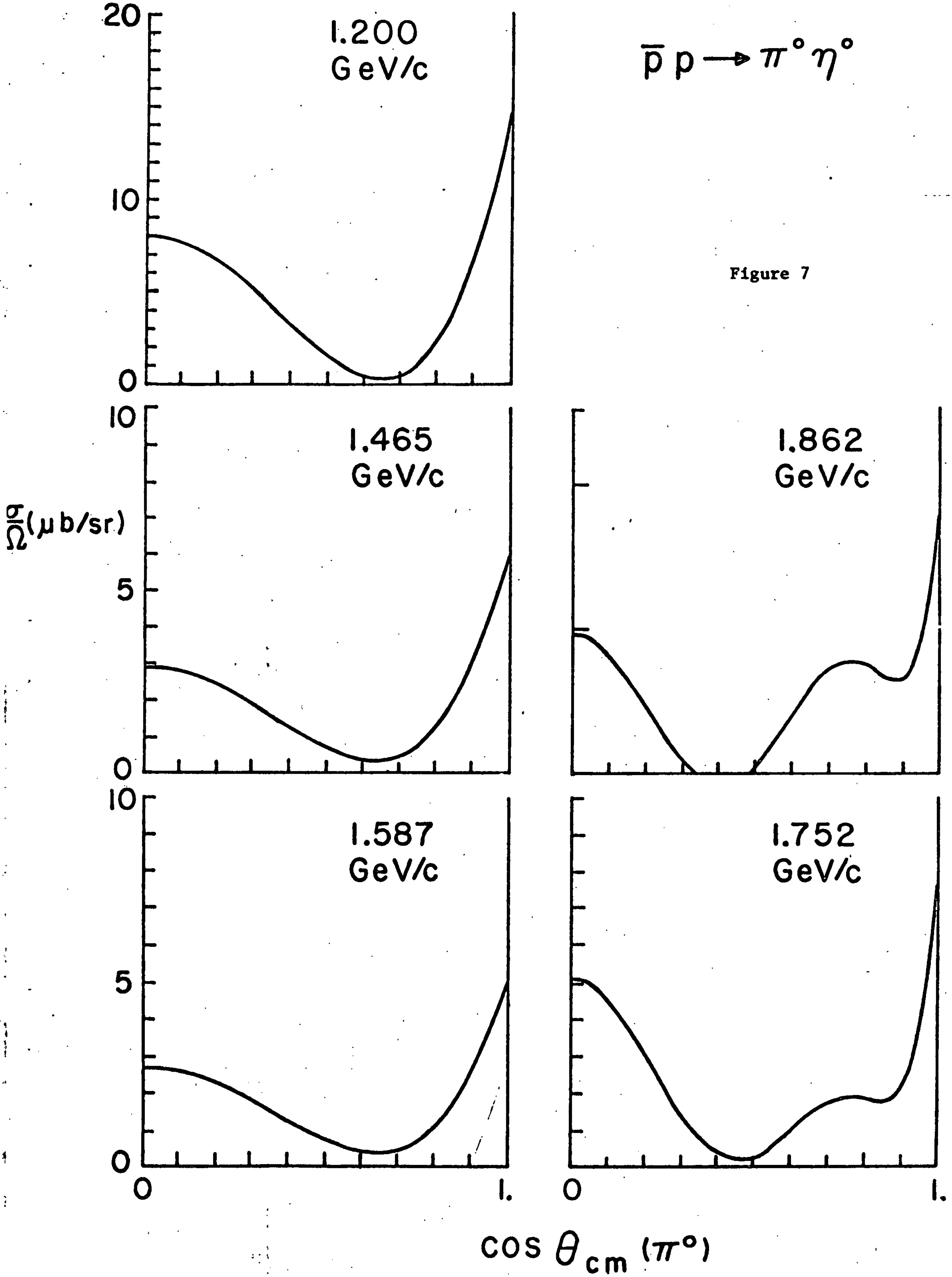

$\bar{p}p \rightarrow \pi^\circ \eta^\circ$
1.200 GeV/c
1.465 GeV/c
1.862 GeV/c
1.587 GeV/c
1.752 GeV/c
$\frac{\sigma}{\Omega}$(μb/sr)
20
10
5
0
1.
cos $\theta_{cm}$ ($\pi^\circ$)


Figure 7

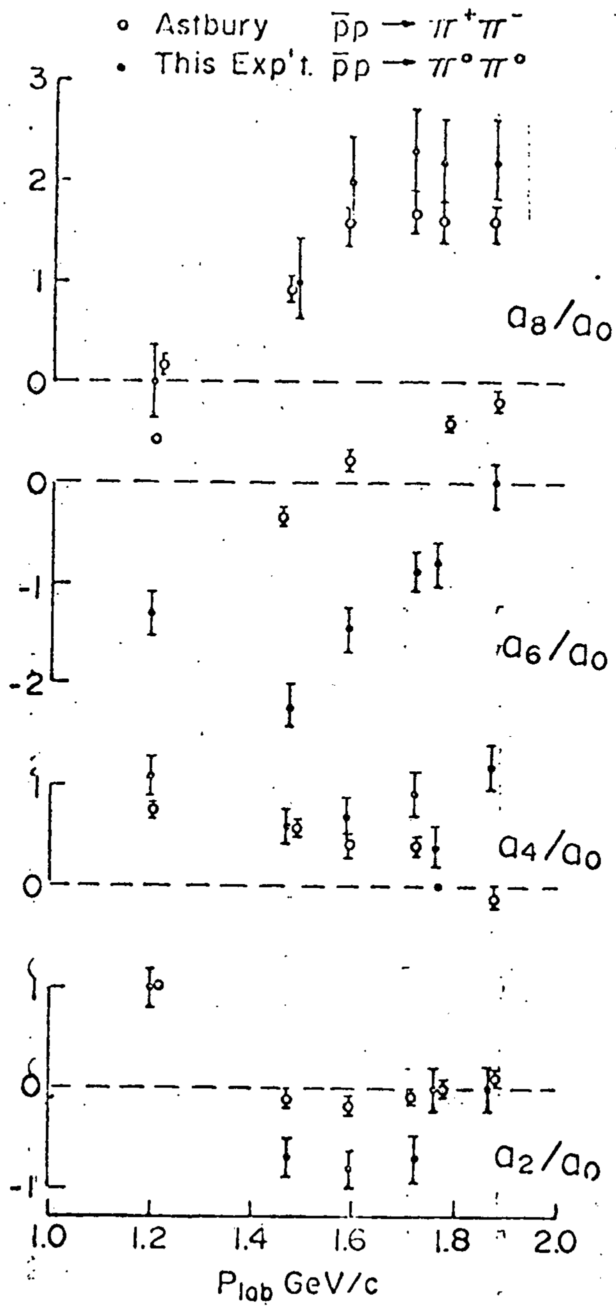


Figure 8 Normalized Legendre coefficients for $\bar{p}p \to \pi^0\pi^0$ and $\bar{p}p \to \pi^+\pi^-$

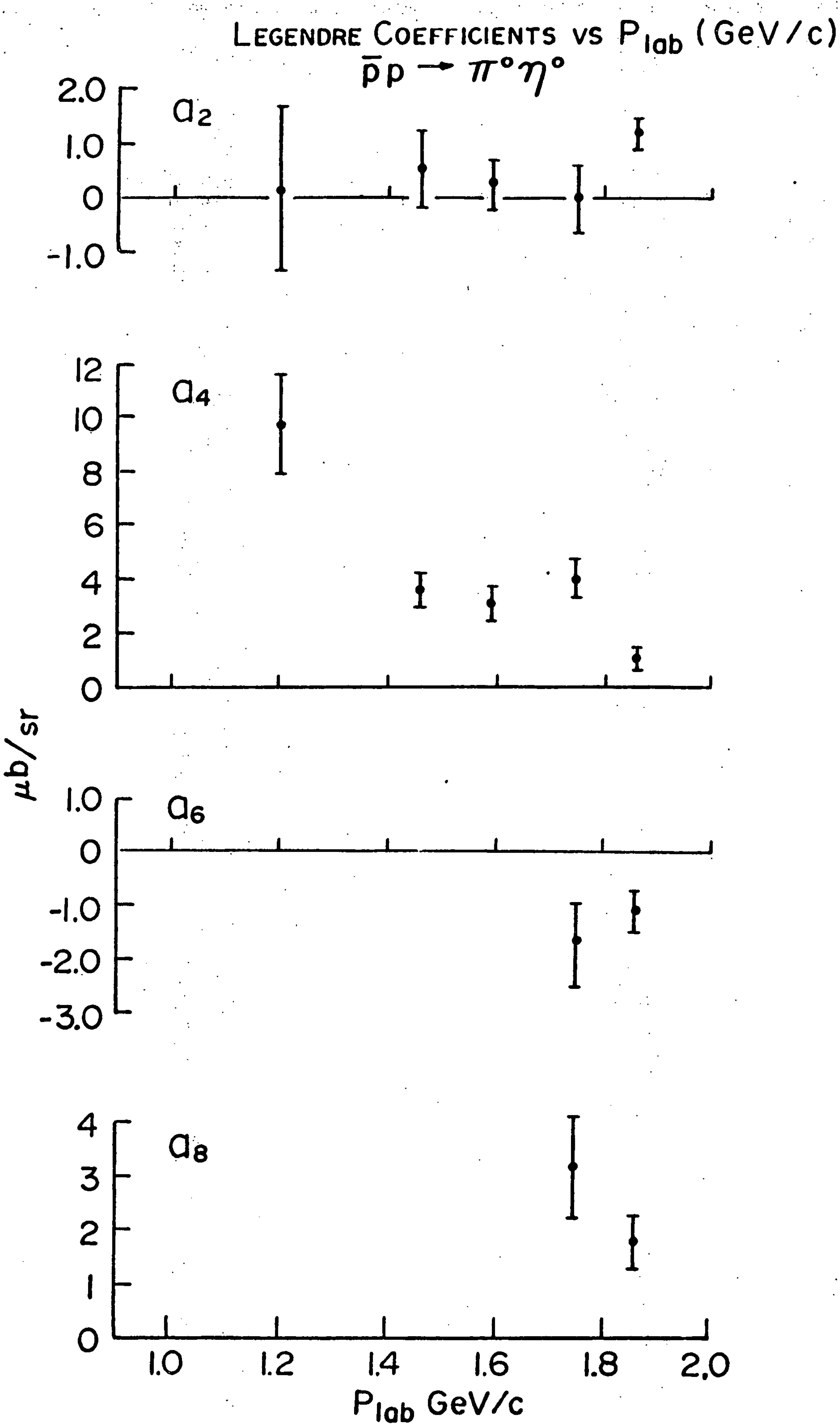

LEGENDRE COEFFICIENTS VS $P_{lab}$ (GeV/c)
$\bar{p}p \rightarrow \pi^\circ \eta^\circ$
$a_2$
2.0
1.0
0
-1.0
$a_4$
12
10
8
6
4
2
0
μb/sr
$a_6$
1.0
0
-1.0
-2.0
-3.0
$a_8$
4
3
2
1
0
1.0
1.2
1.4
1.6
1.8
2.0
$P_{lab}$ GeV/c


Figure 9

Using our data for $\bar{p}p \rightarrow \pi^{\circ}\pi^{\circ}$ it is possible to effect an isotopic spin decomposition of the $\bar{p}p \rightarrow \pi^{+}\pi^{-}$ data. Because of the restrictions of Bose statistics (I+J) must be even for any $\pi\pi$ state. The $\bar{p}p \rightarrow \pi^{+}\pi^{-}$ amplitude is a sum of I = 0 and I = 1 amplitudes of even and odd spherical harmonics respectively. If we expand the differential cross section in Legendre polynomials, the even coefficients are the sum of the isospin amplitudes squared; subtracting the $\bar{p}p \rightarrow \pi^{\circ}\pi^{\circ}$ Legendre coefficients (which are the pure I = 0) leaves the coefficients for the pure I = 1 differential cross section. The odd coefficients represent the interference terms between I = 0 and 1.

We have carried out this separation using the interpolated $\pi^{+}\pi^{-}$ coefficients and the resulting I = 1 coefficients are shown in Figure 10 with the corresponding differential cross sections shown in Figure 11. Since the I = 1 cross section is symmetric about 90° only the forward hemisphere is shown to facilitate comparison with the I = 0 distributions.

The coefficients of both I = 0 and I = 1 seem to vary smoothly throughout this region. If there are any resonant structures lurking in the $\bar{p}p$ system they will have to await more data before they could be untangled. We hope to have much more data analysed in the next year. To achieve this it is very important to keep our scanning staff at the highest possible level since it is the event production rate which is our current limitation.

Our plans for the current year include intensive work on data production. A severe handicap is in scanning manpower, which when the work for AGS Expt #622 (see below) is taken into account, is inadequate to do the job in a reasonable amount of time. We have also suffered from the

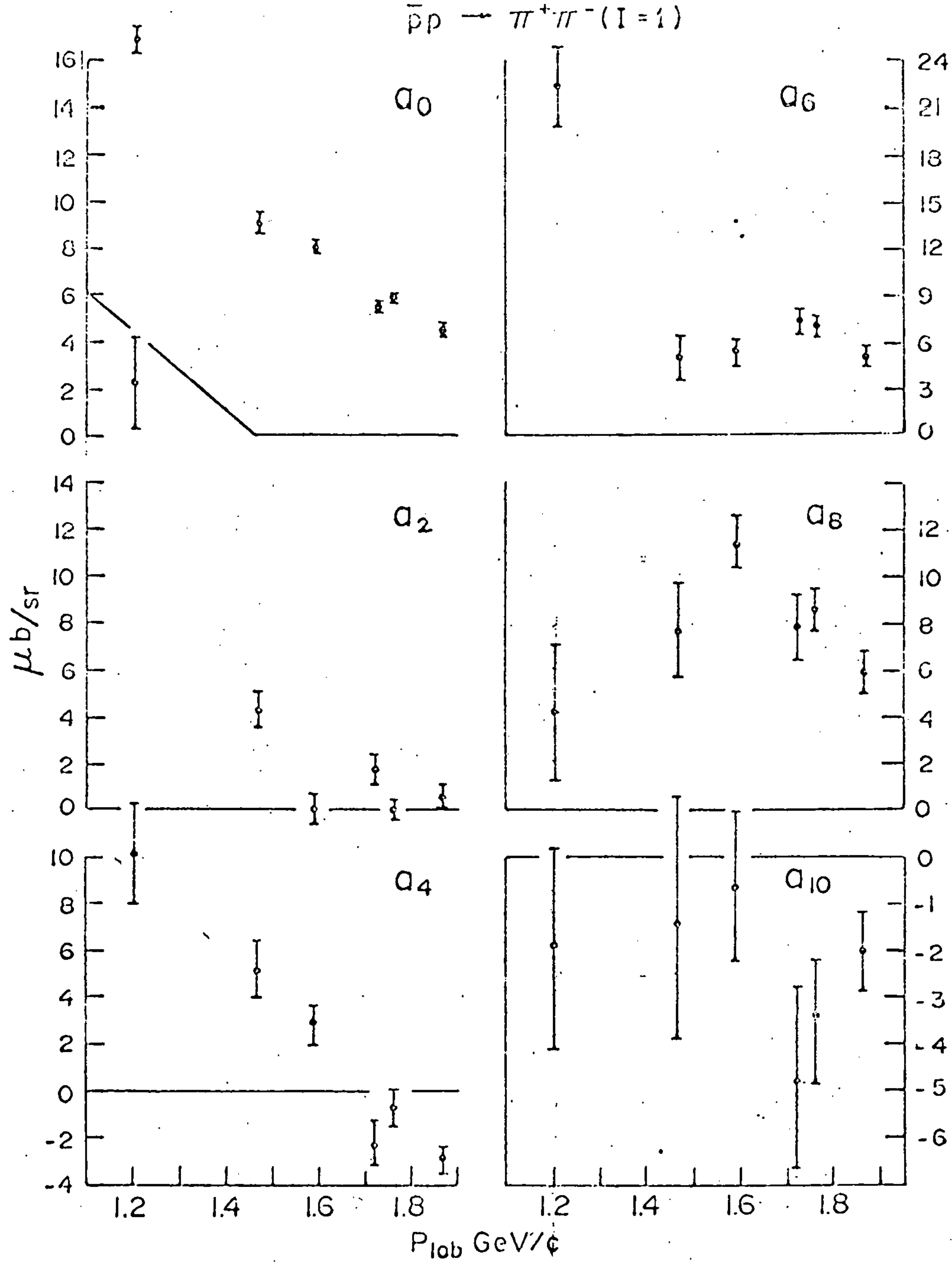


Figure 10 Legendre coefficients for $\bar{p}p \rightarrow \pi^+\pi^-$ in pure I=1 state

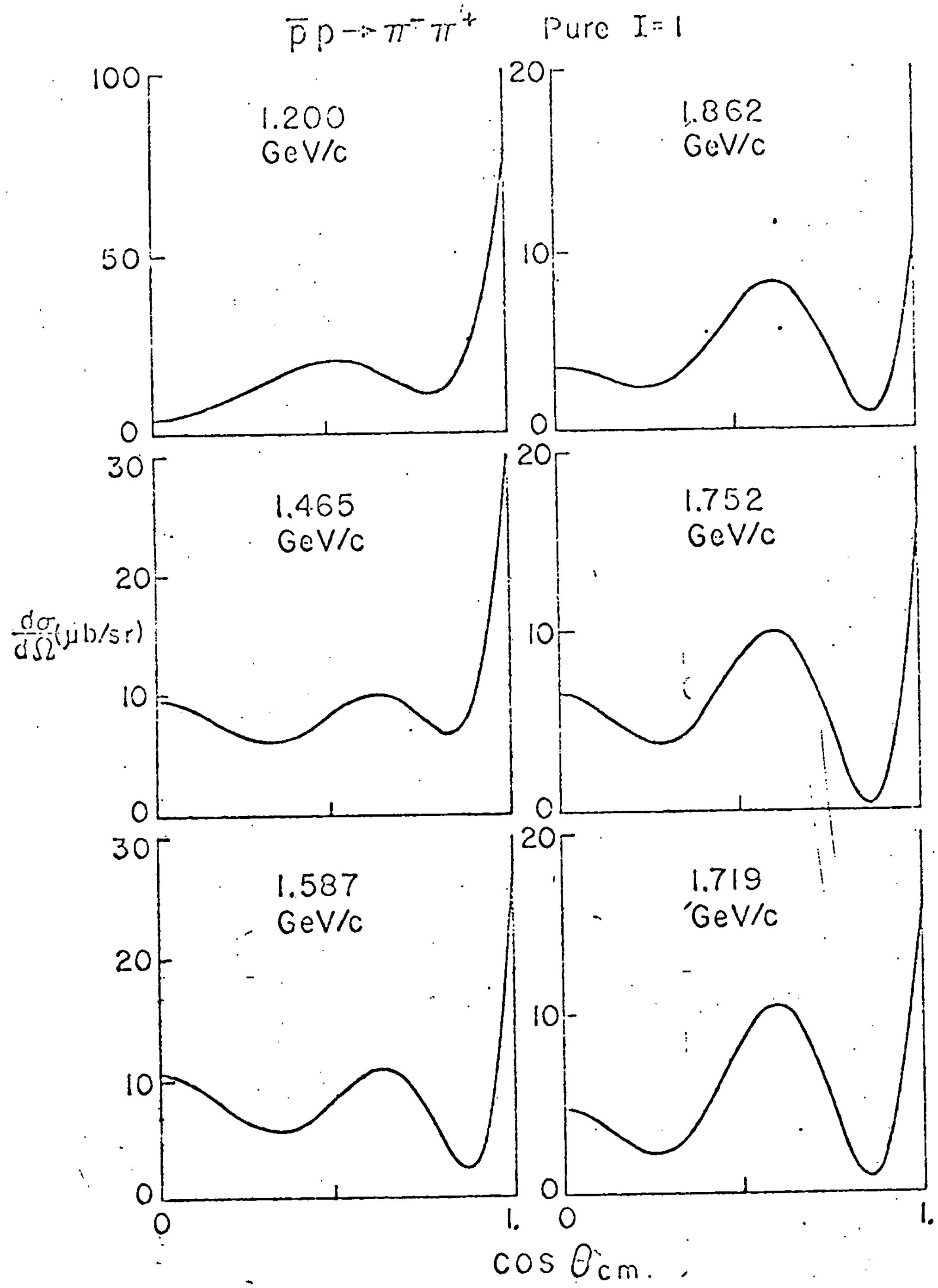


Figure 11 Differential cross sections for $\bar{p}p \to \pi^+\pi^-$ in pure I=1 state.

delay in the replacement of our post doctoral physicist Dr. George Chen. This problem is discussed further in the accompanying Renewal Proposal.

Mr. R. K. Thornton, who was a resident at Brookhaven during the running of this experiment and AGS #622, continues on the data analysis and a portion of the work will serve as the basis of his Ph.D. dissertation.

[11] Esienhandler et al., Phys. Lett. B47, 531, 1973.

[12] See for example invited talk by W. Chinowsky at IV International Conference on Experimental Meson Spectroscopy or B. Richter, Bull. Am. Phys. Soc. 19, 100 (1974).

[13] A. Pais, Phys. Rev. Lett. 32, 1081 (1974).

[14] S. J. Orfanidis and V. Rittenberg, Rockefeller Univ. Pre-print #COO-2232B-8.

c) Search for $\bar{p}p$ Resonances of Definite G-Parity in the T-Region (AGS #622).

As was mentioned last year, the motivation for AGS #622 came largely because of its complementary relation to our AGS #527 and the nature of the currently, somewhat confused situation in high-mass boson spectroscopy (see e.g., Proceedings of Experimental Meson Spectroscopy - 1972, A. I. P. Conference Proceedings No. 8, Rosenfeld & Lai, editors -- subsequent years have not clarified the situation). Briefly the situation is that mesons seen in some types of experiments are not seen in others of a different type (or occasionally even the same type) while some that have been seen via particular decay channels have no unambiguous quantum number assignments.[15] Our AGS #622 is designed to improve the situation in the former while AGS #527 was designed for the latter purpose of unambiguous quantum number assignment.

The principal assumption involved in AGS #622 is that if any resonant $\bar{p}p$ states exist they will be in a state of definite G-parity. We chose the 2190 MeV (T-meson) mass region because of the rather strong evidence there is both a total cross section enhancement as well as a unique channel ($\rho\rho\pi$) enhancement in that vicinity. This region is of course also covered in AGS #527 using our neutral two-body trigger. AGS #622 then consists of a determination with high mass resolution ($\simeq$8 MeV intervals) of the number of even and odd pion final states produced in $\bar{p}p$ annihilation and amounts to a determination of the number of $\pi^\circ$'s produced in the annihilation since the total number of charged mesons is even due to charge conservation. We should be able to detect energy dependent structure at the 2-3% level above background. As was mentioned at the time of the proposal, an interesting by-product of this work will be the first complete determination of the total (i.e., including $\pi^{\circ}$'s) multiplicity distribution of pions in $\bar{p}p$ annihilation as well as a new measurement of $\bar{p}p$ total cross sections with high mass resolution. As was mentioned in the previous section with respect to eta meson production this aspect of the experiment, relating to the $\pi^{\circ}$'s, has taken on a new importance since the interesting new results[12] on $e^+e^- \to$ hadrons being seen on the first experiment at SPEAR. Recall the SPEAR experiments found that only 55% of the total energy in $e^+e^- \to$ hadrons appears in charged particles. The present form of those experiments is such that they are unable to measure $\pi^{\circ}$'s. This becomes extremely important in trying to understand the hadronic part of the $e^+e^-$ single photon annihilation[13] diagram. To do this, it becomes important to know how this "neutral" energy is distributed. The $\bar{p}p$ system is a purely hadronic one with quantum numbers the same as the $e^+e^-$ system. Models for understanding the hadronic part of $e^+e^-$ must simultaneously handle these $\bar{p}p$ states.[14] Although the center of mass energy in AGS #622 is somewhat lower than in the SPEAR experiment the data in the film of #622 are directly applicable to this problem and so far as is known are the only data in existence involving direct detection of individual gammas from which parentage can be inferred.

It will be recalled that our plan last year was to do only scanning and no measuring on the film since we did not require measuring for the G-parity resonance portion of the experiment. We had quite complete scanning information on two rolls of film but we deferred any further production scanning in order to devote our limited scanning power to AGS #527. Instead we have shipped a large portion of this film to one of our collaborators, Professor D. C. Peaslee, at the Australian National

University in Canberra where he has recently set up a scanning group. It is our hope that we will thereby keep data production on a manageable time scale. The results so far look very promising in that annihilation events are rather clearly separable from $\bar{p}p \rightarrow \bar{n}n$ or $\bar{n}n(k\pi^{\pm}_{0})$ events and that the topology identification is relatively clear. This is quite adequate for the G-parity part; however, some measuring may have to be done in order to look at the "neutral" energy part -- in any case, more scanning power is needed if both #527 and #622 are to be completed in less than an additional two years.

Also mentioned last year was our plan to extract from this run a total cross section measurement which complements the classical Abrams et al. experiment,[16] by virtue of the fact that AGS #622 has better mass resolution by about a factor of five, finer mass (or incident momentum) steps but somewhat poorer statistics on the individual points. These features are important because they permit the elimination or possible identification of fine structure in the total cross section at a level of less than half a percent variation from the smooth Abrams curve. This point has taken on additional impetus with the discovery of the well-known Ψ-J-particle, and the suggestion of lower mass states from quark and dual[19] theories, as well as new emulsion results from FNAL.[17] We have now completed this measurement and the results have been reported in a paper accepted for publication (Ref. 212).

A special feature of our result is that unlike production experiments (such as in missing mass spectrometers) which measure only the product of a <u>total</u> width and a production cross section we are able to extract the <u>partial</u> width - cross section product as it relates to the $\bar{p}p$ channel of a possible resonance coupled to bosons.

In what follows we present a brief summary of our result. Figure 12 shows the experimental layout to illustrate how the high mass resolution is achieved by a hodoscope tagging scheme. We have binned our data in 40 MeV/c momentum bins to make a direct comparison with the high statistics measurement of the $\bar{p}p$ cross section made by Abrams et al., (Fig. 13a). The agreement is well within our 3% systematic uncertainty; however, the broad enhancement appears in our data at a higher momentum than that observed by Abrams. To verify this we calculated the $\chi^2$ of our data fit to Abrams as a function of momentum scale shift and absolute normalization (Fig. 14). The shape agreement is quite good with a relative momentum scale change of 3% (Fig. 13b). This is outside our momentum uncertainty of 1.5% and Abrams' uncertainty of 0.5%. The basic conclusions we draw from our experiment are unaffected by this apparent momentum scale discrepancy.

In Fig. 15 we present the cross sections in 6.5 MeV/c momentum bins (2.25 MeV in mass). Each data point typically contains contributions from three hodoscope measurements. Using our fit through the data points (Fig. 15) we performed several statistical tests to determine if any apparent structure was significant. The most sensitive indicator was related to a test for auto-correlation designed by Durbin and Watson[18] and is given by

$$d = \sum_{i=2} u_i u_{i-1} / \sum_{i=1} u_i^2$$

where $u_i$ is the residual of data point i from the smooth fit . We compared the value of d from our data with values tabulated by Durbin and Watson and also with data simulated by a sample of residuals picked randomly from a Gaussian distribution. These tests showed that any structure observed in our data can be understood on the basis of statistical effects. We paid

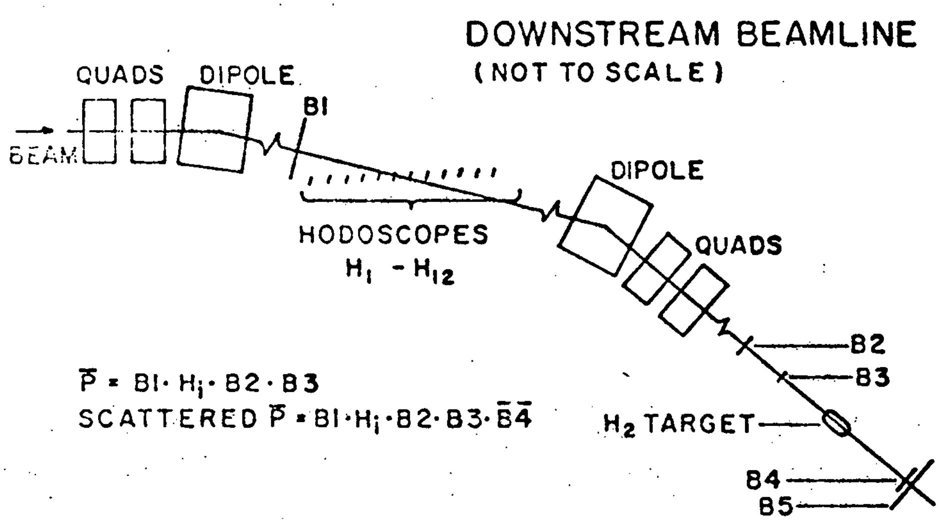


Figure 12

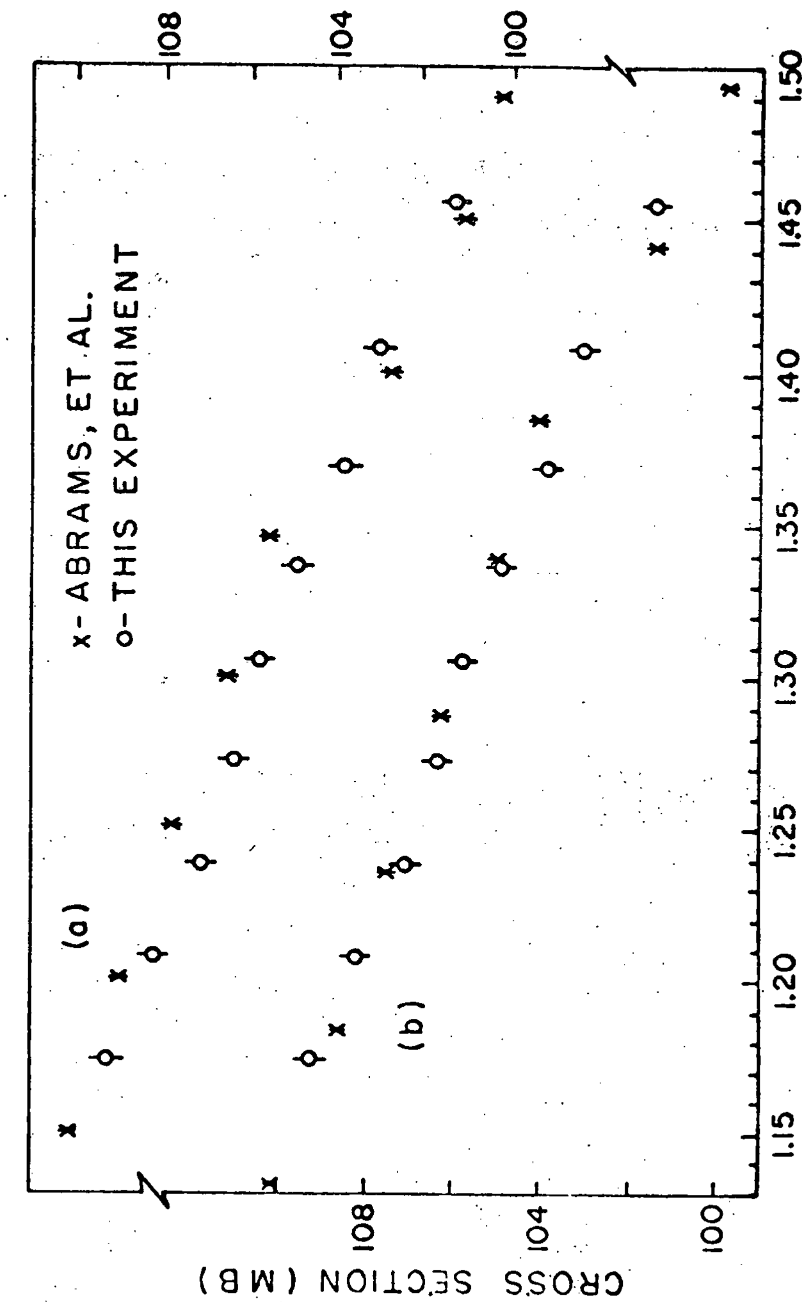


Figure 13

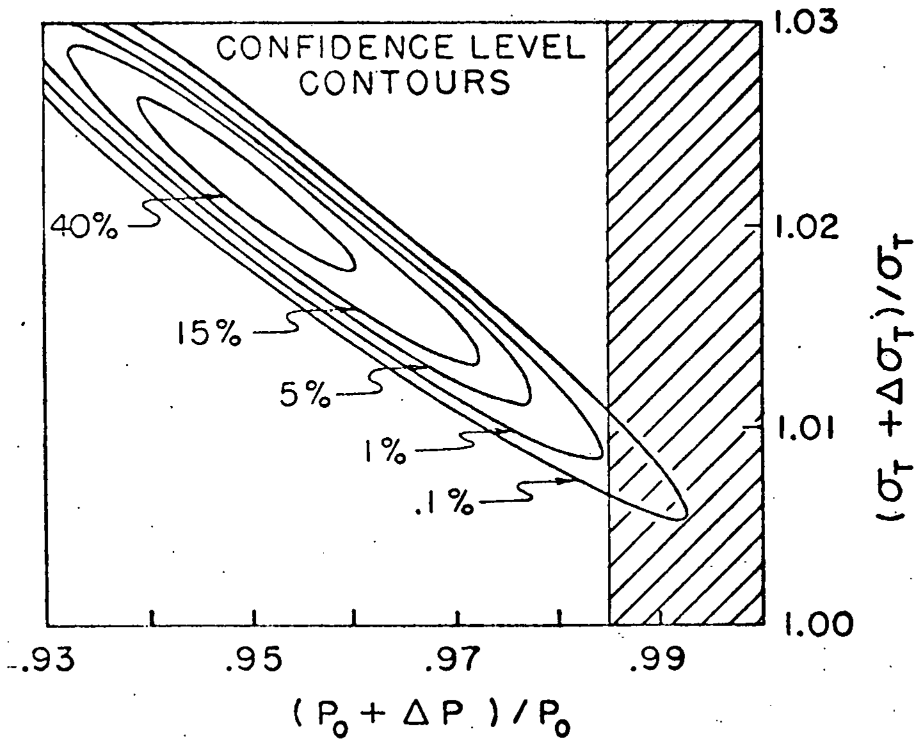


**Figure 14**

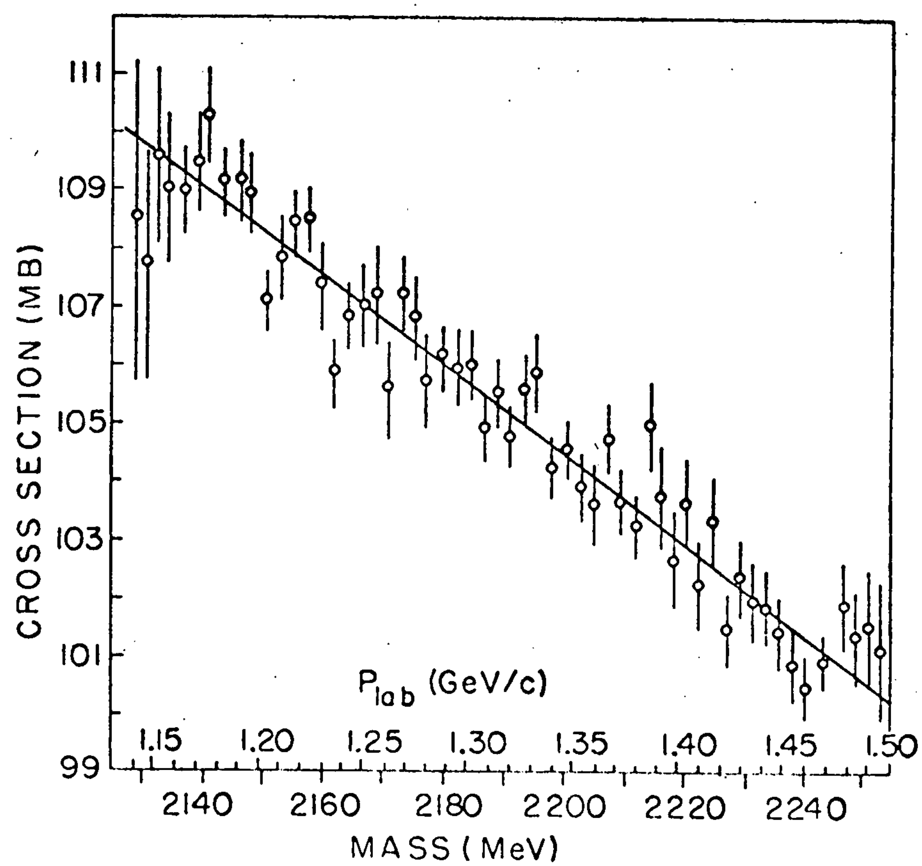


**Figure 15**

particular attention to the fluctuation at 1.22 GeV/c. Our tests were performed in this region alone and produced a 2 standard deviation effect. It would take a measurement with more than four times our statistics to make a conclusive statement about a structure of this size. In this connection it should be remarked that tests for Ericson fluctuations in these data require very high statistics due to the large number of states accessible to the $\bar{p}p$ system.[20]

Our data (Fig. 15) exclude the existence of resolution sized structure above the smooth fit with the product of cross section and width greater than 7 MeV mb. (Limits on larger width structures may be obtained by multiplying 7 MeV mb. by the square root of the number of data points needed to span the width.) From this it can be shown that a Breit-Wigner resonance of spin J coupled to the $\bar{p}p$ system in this region must have partial width $\Gamma_{pp}$ less than 1.8/(2J + 1) MeV. The spin states available to the $\bar{p}p$ system at incident momentum 1.3 GeV/c might be expected to be restricted by impact parameter considerations to $J \lesssim 5$. It is of interest to note that while this sets a rather stringent limit (e.g., partial width for decay of a spin 5 object to $\bar{p}p$ is less than 165 keV) on a massive, high spin resonance; it does not exclude the type of event of mass 2.2 GeV reported as seen in emulsion stacks exposed to 205 GeV protons at FNAL.[17] Furthermore we find that the broad (85 MeV) enhancement observed in the $\bar{p}p$ cross section persists without modification in an observation with mass resolution 6 times that of Abrams et al.

15 W. A. Cooper et al., Phys. Rev. Lett. 20, 1059 (1968).
G. Kalbfleisch et al., Phys. Lett. 29B, 259 (1969).
P. Yamin et al., Bull. Am. Phys. Soc. 18, 125 (1973).
R. Donald et al., Nucl. Phys. B61, 333 (1973).
R. Donald et al., Phys. Lett. 40B, 586 (1972).

16 Abrams et al., Phys. Rev. D1, 1917, (1970); also see Alspector et al., Phys. Rev. Lett. 30, 511, (1973).

17 Hoshino et al., Nagoya University Report #DPNU-3 (1975).

18 J. Durkin and G. S. Watson, Annals of Math. Statistics 22, 446, (1951).

19 For reviews of these predictions see A. Astbury, in CERN Report No. 74-18, 1974 (unpublished), p. 46, or R. H. Dalitz, in Experimental Meson Spectroscopy-1974, AIP Conference Proceedings No. 21, Particles and Fields Subseries No. 8, edited by D. A. Garelick (American Institute of Physics, New York, 1974), p. 75.

20 See for example S. Frautschi, Nuovo Cimento 12A, 133 (1972).

d) A Nucleon-Nucleon and Meson-Nucleon Interaction Experiment Using Counter-Spark Chambers at FNAL (FNAL #96).

This experiment (whose data taking runs were recently completed) is to measure elastic scattering and quasi-two-body elastic scattering of $K^+$, $K^-$, p, and $\bar{p}$ on hydrogen and deuterium (neutron) targets up to 200 GeV/c incident momentum and at $|t|$ values of .04 to 1.2 $(GeV/c)^2$. It has been described extensively in previous Progress Reports and Renewal Proposals.

The spectrometer (which has been adopted as a facility by FNAL) is of flexible design and can operate either with 8μ steradians acceptance and ±0.03% momentum precision up to 200 GeV/c or can be changed to give considerably larger acceptance at lower momenta. It is equipped with differential and threshold Cerenkov counters as well as scintillation counters, hodoscopes, and multi-wire proportional chambers. The collaboration assembled to construct and carry out this experiment consisted of individual physicists from ANL, Bari, Brown, CERN, Cornell, MIT, Stanford, and FNAL.

During the past year the experiment has completed data taking. This was accomplished during a series of three 6-8 week running periods during last August, again in October, and finally in January. Running at FNAL ended on 18 February. During this period gradual improvements were made to the spectrometer, for example a significant narrowing of our resolution was achieved by the addition of new voltage stabilization on several of the trim and bend magnets. Such improvements are a continuing process on the spectrometer .

In the course of the entire experiment approximately 400 raw data tapes were written containing about $12 \times 10^6$ events. Analyses of these data have been underway at Brown, Cornell, FNAL, MIT, and SLAC. Preliminary results, chiefly related to the important question of asymptotic behaviour of slopes of $d\sigma/dt$ at small momentum transfer in elastic scattering, have been reported by ourselves and collaborators in invited papers at XVII International Conference on High Energy Physics (London), the annual meeting of the APS (Anaheim), and X Rencontre de Moriond (Phenomenology of Hadronic Structure) at Meribel, France.

These results are contained in the accompanying Tables and Figures.

1) Figure 16 is a typical missing mass plot which serves to illustrate the quality of the data and the relative separation of the elastic peak from the background.

2) Figure 17 is a typical differential cross section for these elastic data.

3) Table 2 gives a tabulation for the slope parameters for all particles and all energies.

4) Figure 18 shows the dependence of $B_{EFF}(|t| = 0.2\ GeV/c^2)$ on the energy variable s for our data combined with Serpuhkov and ISR data.

Our differential cross sections in the t-range from -0.04 to -0.8 $(GeV/c)^2$ are well represented by the expression

$$\frac{d\sigma}{dt} = A \exp(-B|t| + C|t|^2)$$

It has become conventional in many experiments of this sort to make inter-experiment comparisons independent of parameterization in t by comparing $B_{EFF}$ at $t = -0.2\ (GeV/c)^2$. Where $B_{EFF}$ is given as equal to $B + 2C|t|$, that is, the logarithmic derivative. The only experiments available for comparison are the Serpuhkov experiments[22,23] at 50 GeV/c for mesons and nucleons and protons at FNAL.[21] The agreement at this point is very good.

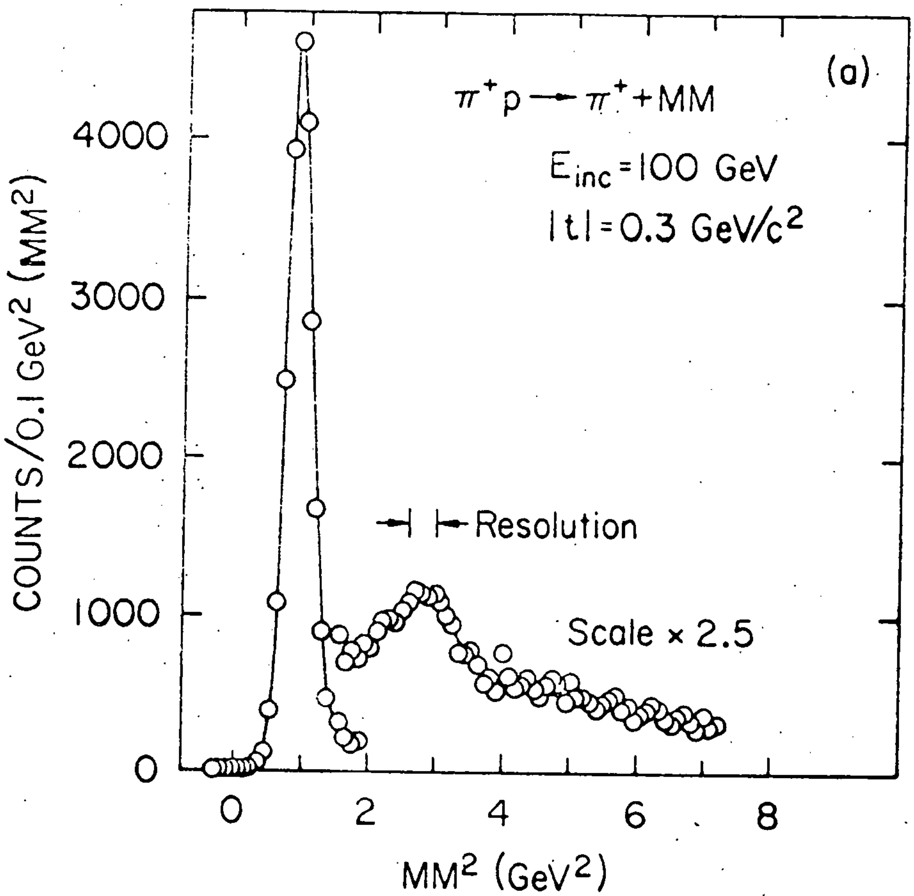


Figure 16

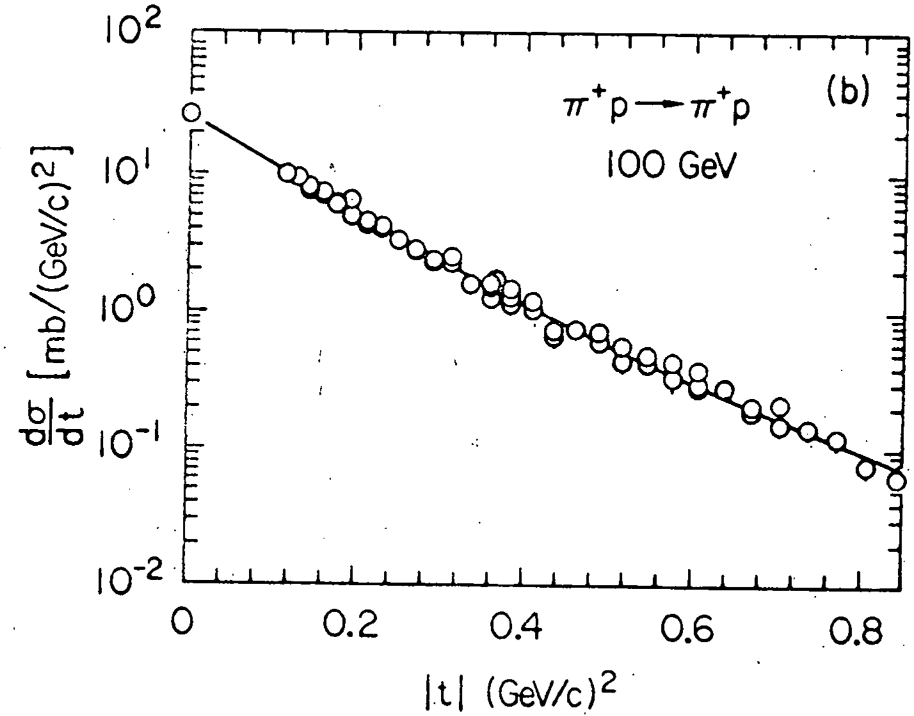


Figure 17

Table 2. Preliminary results from E96

| | E | $A \pm \delta A$ | $-B \pm \delta B$ | $C \pm \delta C$ | $-B_{eff} \pm \delta B_{eff}$ |
|---|---|---|---|---|---|
| $\pi^+ p$ | 50 | 27.9 ± 0.4 | 8.87 ± 0.12 | 1.9 ± 0.2 | 8.11 ± 0.17 |
| | 70 | (data not yet analysed) | | | |
| | 100 | 27.5 ± 0.7 | 8.81 ± 0.17 | 2.1 ± 0.2 | 7.97 ± 0.20 |
| | 140 | 27.9 ± 0.5 | 8.36 ± 0.12 | .79± 0.2 | 8.04 ± 0.17 |
| | 175 | (data not yet analysed) | | | |
| $\pi^- p$ | 50 | 32.0 ± 0.4 | 9.87 ± 0.10 | 3.2 ± 0.1 | 8.60 ± 0.17 |
| | 70 | (data not yet analysed) | | | |
| | 100 | 27.4 ± 0.5 | 9.04 ± 0.13 | 2.4 ± 0.2 | 8.10 ± 0.18 |
| | 140 | 23.9 ± 0.5 | 9.19 ± 0.15 | 2.4 ± 0.2 | 8.25 ± 0.18 |
| | 175 | (data not yet analysed) | | | |
| $K^+ p$ | 50 | 17.1 ± 0.4 | 6.94 ± 0.29 | 0.3 ± 0.6 | 6.81 ± 0.24 |
| | 70 | (data not yet analysed) | | | |
| | 100 | 18.1 ± 0.5 | 7.81 ± 0.32 | 1.9 ± 0.5 | 7.05 ± 0.27 |
| | 140 | 18.8 ± 0.5 | 7.94 ± 0.20 | 1.1 ± 0.4 | 7.51 ± 0.21 |
| | 175 | (data not yet analysed) | | | |
| $K^- p$ | 50 | 21.1 ± 0.6 | 8.80 ± 0.31 | 2.3 ± 0.6 | 7.87 ± 0.26 |
| | 70 | (data not yet analysed) | | | |
| | 100 | 20.9 ± 0.6 | 9.13 ± 0.34 | 3.1 ± 0.6 | 7.88 ± 0.27 |
| | 140 | 21.7 ± 0.5 | 8.99 ± 0.27 | 2.4 ± 0.6 | 8.03 ± 0.23 |
| | 175 | (data not yet analysed) | | | |
| $p^+ p$ | 50 | 75.4 ± 0.7 | 10.28 ± 0.11 | 1.4 ± 0.2 | 9.75 ± 0.17 |
| | 70 | (data not yet analysed) | | | |
| | 100 | 75.6 ± 1.5 | 10.96 ± 0.17 | 2.0 ± 0.3 | 10.15 ± 0.19 |
| | 140 | 75.6 ± 1.2 | 11.30 ± 0.12 | 2.5 ± 0.2 | 10.33 ± 0.17 |
| | 175 | (data not yet analysed) | | | |
| $\bar{p}p$ | 50 | 100.2 ± 1.7 | 12.75 ± 0.22 | 3.2 ± 0.5 | 11.50 ± 0.20 |
| | 70 | (data not yet analysed) | | | |
| | 100 | 92.0 ± 2.4 | 12.39 ± 0.34 | 3.9 ± 0.7 | 10.82 ± 0.27 |
| | 140 | 88.3 ± 2.2 | 12.77 ± 0.50 | 4.4 ± 1.5 | 11.03 ± 0.29 |
| | 175 | (data not yet analysed) | | | |

$$\frac{d\sigma}{dt} = A\, e^{-B|t|+C|t|^2}$$

$$B_{eff} = B + 2C|t|$$

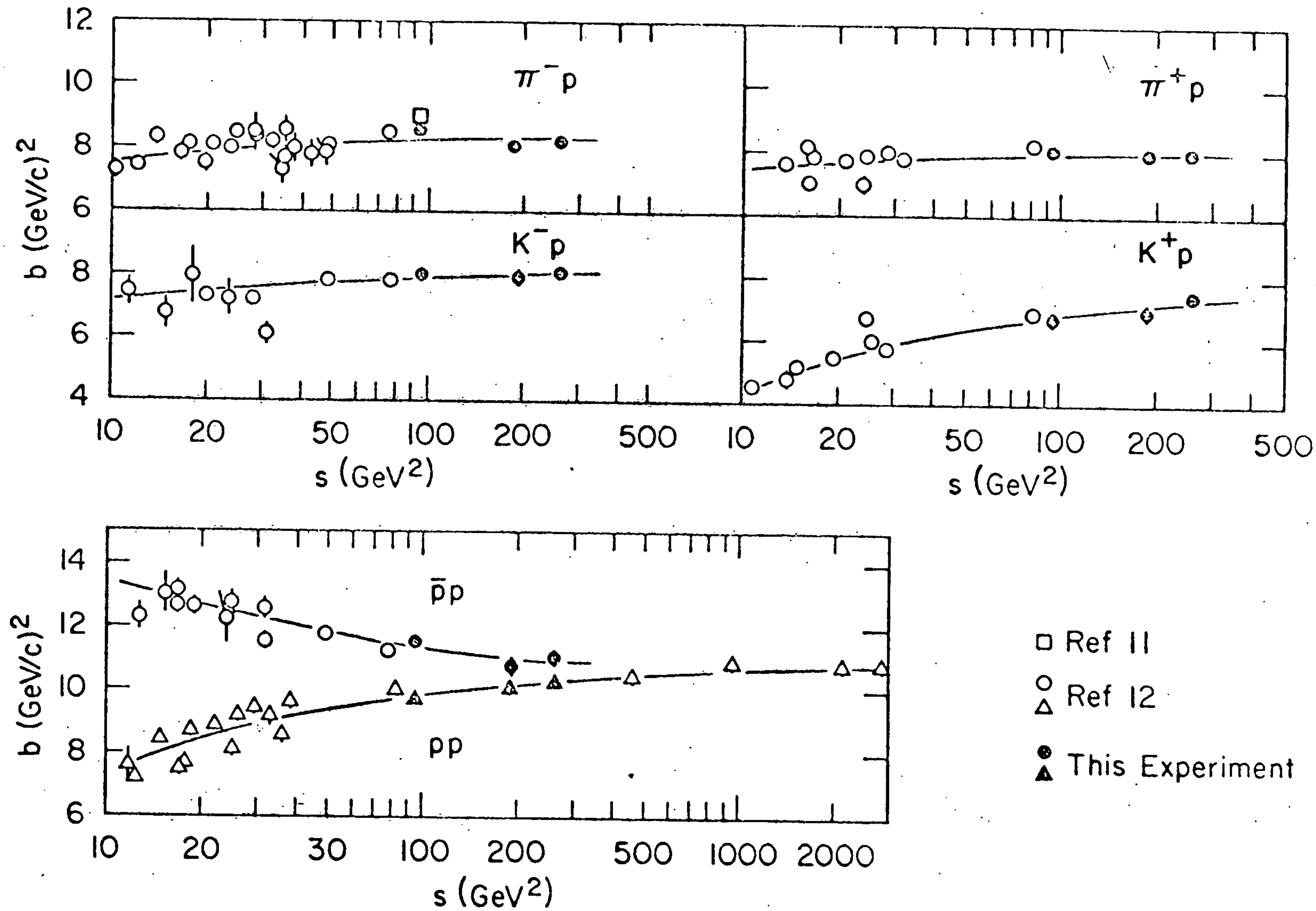
b (GeV/c)$^2$
$\pi^-p$
$\pi^+p$
$K^-p$
$K^+p$
s (GeV$^2$)
$\bar{p}p$
pp
Ref 11
Ref 12
This Experiment

Figure 18

The rest of our data is of course completely new since mesons and antiprotons at these energies have not been available previously. As expected the angular distributions are rather featureless but the behaviour of the slopes as a function of s is rather interesting. In particular, the pions seem to have reached essentially constant slopes whereas the kaons indicate the $K^-$ behaves similarly to the pions while the $K^+$ is still rising. The proton and antiproton appear to be both approaching the same constant value at an s of about 400. While direct and complete comparison with regge and geometric models will have to await our final evaluation of total elastic, total and inelastic cross sections it is already apparent that there will be discrepancies. A very preliminary attempt at evaluating these cross sections is shown in Table 3 and the resulting energy indepence shown for $K^+p$ is in direct contradiction with the current version of the theory of Chen and Wu [24] as well as that of Sidhu and Wang.[25]

A paper is in preparation on these results as they relate to slope determination.

A considerable amount of analysis work remains on differential cross section cross-over, total elastic cross sections, quasi-elastic distributions, and deuterium data related to all of the above.

The experiment has turned out to produce very high quality data and appears to be capable of producing copious results in several areas. We look forward to more interesting results in this entirely new range of projectiles and momenta.

Mr. Lorne Levinson, part of whose Ph.D. thesis will contain data from this experiment, has returned to Brown from full-time residence at FNAL. He has undertaken responsibility for the major portion of the deuterium analysis. He presented a paper (Ref. 213) at the Washington A.P.S. meeting

Table 3. Preliminary E96 cross sections

| | p GeV/c | $\sigma_{el}$ | $\sigma_{inel}$ | $\sigma_{tot}$ |
|---|---|---|---|---|
| $\pi^-p$ | 50 | 3.46 ± .07 | 20.97 ± .11 | 24.43 ± .09 |
| | 100 | 3.32 ± .09 | 20.39 ± .13 | 23.71 ± .10 |
| | 140 | 3.41 ± .18 | 20.59 ± .21 | 23.99 ± .11 |
| $K^-p$ | 50 | 2.59 ± .16 | 17.66 ± .18 | 20.25 ± .09 |
| | 100 | 2.54 ± .19 | 17.81 ± .21 | 20.36 ± .10 |
| | 140 | 2.59 ± .15 | 17.94 ± .18 | 20.52 ± .10 |
| $\bar{p}p$ | 50 | 8.10 ± .19 | 35.71 ± .28 | 43.81 ± .21 |
| | 100 | 8.04 ± .37 | 34.08 ± .47 | 42.13 ± .30 |
| | 140 | 7.39 ± .53 | 34.29 ± .57 | 41.68 ± .20 |
| $\pi^+p$ | 50 | 3.31 ± .08 | 19.86 ± .13 | 23.17 ± .10 |
| | 100 | 3.34 ± .10 | 19.93 ± .15 | 23.27 ± .11 |
| | 140 | 3.44 ± .08 | 20.02 ± .12 | 23.46 ± .10 |
| $K^+p$ | 50 | 2.48 ± .13 | 15.57 ± .15 | 18.06 ± .08 |
| | 100 | 2.51 ± .18 | 16.36 ± .20 | 18.87 ± .09 |
| | 140 | 2.49 ± .10 | 16.90 ± .14 | 19.39 ± .10 |
| pp | 50 | 7.57 ± .16 | 30.90 ± .20 | 38.47 ± .12 |
| | 100 | 7.21 ± .19 | 31.30 ± .27 | 38.51 ± .19 |
| | 140 | 7.01 ± .14 | 31.56 ± .22 | 38.57 ± .17 |

$$\sigma_{el} \equiv \int_0^{|t|\sim 1.0} \left(\frac{d\sigma}{dt}\right)_{el} dt \quad ; \quad \text{with } \left(\frac{d\sigma}{dt}\right)_{el} = A\, e^{B|t|+Ct^2} \quad ;$$

$$\sigma_{tot} \equiv 4.424 \left[\frac{d\sigma}{dt}\bigg|_{t=0}\right]^{\frac{1}{2}} = 4.424 \times A^{\frac{1}{2}} \quad ;$$

$$\sigma_{inel} = \sigma_{tot} - \sigma_{el} \quad .$$

on some of the on-line software work done at Brown primarily for E96 but which has aroused much user interest. The system developed is now in use at FNAL generally, and in addition at BNL, Berkeley and SLAC.


[21] V. Bartenev et al., Phys. Rev. Lett. 31, 1088 (1973).

[22] A. Derevchekov et al., Phys. Lett. B48, 367 (1974).

[23] Y. Antipov et al., Nucl. Phys. B57, 333 (1973).

[24] Cheng et al., NAL-Pub-74/52 (1974).

[25] Sidhu et al., Phys. Rev. 11D 1354 (1975).

## II. Experimental Runs in Progress and in Preparation.

### An Experiment to Study "Inclusive" Reactions Using the NAL Single-Arm Spectrometer (FNAL #118).

Last November the FNAL Program Committee approved our proposal to study inclusive reactions including particle multiplicity detection. The experiment is now scheduled for testing in late summer and early fall with running to begin as soon as possible.

We proposed to make an experimental study of the so-called "inclusive reactions" -- they are ones in which some particles or property of the final state is studied without trying to specify what else is happening in the reaction -- these reactions are usually represented by $a + b \rightarrow c + \text{anything}$. More specifically, we plan to make an exploratory investigation of these processes by measuring the momentum spectra of final state hadrons over a range of production angles and incident energies with the use of the FNAL focussing spectrometer which has been constructed for Experiment #96, as mentioned above. By employing an array of Cerenkov counters in the spectrometer set to be sensitive to different masses, the momentum distribution of protons, $\pi^+$, and $K^+$ can be simultaneously measured. The spectra of final state $\pi^-$, $K^-$, and $\bar{p}$ can be simultaneously measured with reverse magnetic fields. With the use of Cerenkov counters in the incident beam as well, reactions resulting from protons, anti-protons, $K^{\pm}$ mesons, and $\pi^{\pm}$ mesons can be simultaneously measured over the part of the kinematic range to be covered in this experiment in which incident intensities are about $10^7$ particles per pulse or less. Multiwire proportional chambers and segmented, lucite Cerenkov counters surround the target and give the particle multiplicity for each event. Some further design work on this part of the apparatus has been done this year.

Intensive work was begun at Brown, as soon as approval was given, on several items. An update and re-formulation of the on-line software is under the direction of Professor Massimo. The design and creation of a rapid, off-line physics analysis program suitable for use at FNAL during running periods is being supervised by Professor Cutts. A design for a re-configuration of the beam line and spectrometer to optimize them for this experiment has been undertaken by Professor Lanou. Electronics for the MWPC are also being constructed here as per a design from our Bari collaborators. Much work remains to be done as is discussed further in our Renewal Proposal.

III. Associated Matters.

Professor Cutts was an invited speaker at a conference on "Phenomenology of Hadronic Structure" at the Xth Rencontre de Moriond held in Meribel, France and sponsored by Orsay and Saclay. He presented our results from E96 at FNAL.

Professor Lanou attended the XVII International Conference on High Energy Physics held in London last summer. He represented the Brown experimental groups and presented data from our AGS #527 experiment on $\bar{p}p \rightarrow \pi^\circ\pi^\circ$.

Mr. Ronald Thornton gave an invited paper at the IVth International Symposium on Nucleon-Antinucleon Interactions held in Syracuse, N. Y. in May. He spoke about the $\bar{p}p \rightarrow \pi^\circ\eta^\circ$ and $\eta^\circ\eta^\circ$ results from AGS #527.

Professor Lanou was elected chairman of the Nominating Committee of the HEDG organization at the Brookhaven National Laboratory. Other members of the committee are E. Beier (Penn.), W. Carrithers (Rochester), K. Foley (BNL), and M. Good (Stony Brook).

Professor Massimo has been promoted to the rank of full professor.

## IV. Scientific Personnel Associated with the Counter-Spark Chamber Program.

| | | |
|---|---|---|
| R. E. Lanou, Jr. | -- | Professor |
| J. T. Massimo | -- | Professor |
| D. Cutts | -- | Assistant Professor |
| G. T. Chen replacement | -- | Research Associate |
| R. K. Thornton | -- | Graduate Research Assistant |
| L. J. Levinson | -- | Graduate Research Assistant |

C. Papers Published During the Preceding Year and Papers in Press.

192. D. G. Fong, M. Heller, A. M. Shapiro, M. Widgoff, and co-authors, "150 GeV/c $\pi^-p$ Interactions in the FERMILAB 30-inch Bubble Chamber-Proportional Wire Chamber Hybrid System," AIP Conference Proceedings of the Williamsburg Meeting (1974) (to be published).

193. D. G. Fong, A. M. Shapiro, and co-authors, "An Improved 30" B.C.-Hybrid System," PHS Consortium Note, Internal Report #132, September 1974.

194. R. Simard, "Strange Particle Final States in $\pi^+p$ Interactions at 4.09 GeV/c," Ph.D. Thesis, Internal Report #133, October 1974.

195. D. G. Fong, "A Brief Description of TRACK ORGANIZER and the Meaning of MULT on the DST," PHS Consortium Note, Internal Report #134, December 1974.

196. D. G. Fong, M. Heller, A. M. Shapiro, M. Widgoff, and co-authors, "Topological and Leading Particle Cross Sections for 147 GeV/c $\pi^-p$ Interactions," Physics Letters 53B, 290 (1974).

197. M. Heller, A. M. Shapiro, and co-authors, "Charged Prong Multiplicities Produced by 147 GeV/c $K^-$ Incident on Protons," B.A.P.S. 20, 14 (1975).

198. D. G. Fong, M. Heller, and co-authors, "Two-Body Correlations among Mesons Produced by 147 GeV/c $\pi^-p$ Interactions," B.A.P.S. 20, 14 (1975).

199. A. M. Shapiro, M. Widgoff, and co-authors, "t Dependence of the Leading Particles in the 2, 4, and 6-Prong Final States Produced by 147 GeV/c $\pi^-p$ Interactions," B.A.P.S. 20, 14 (1975).

200. D. G. Fong, M. Widgoff, and co-authors, "Feynman-x and Rapidity Distributions of $\pi^-$ and $\pi^+$ Mesons Produced by 147 GeV/c $\pi^-p$ Interactions," B.A.P.S. 20, 14 (1975).

201. M. Heller, A. M. Shapiro, and co-authors, "Topological Cross Sections for $\pi^-p$ Interactions at 147 GeV/c," B.A.P.S. 20, 546 (1975).

202. D. G. Fong, M. Widgoff, and co-authors, "Diffractive Excitation in 147 GeV/c $\pi^-p$ Collisions," B.A.P.S. 20, 546 (1975).

203. D. G. Fong, M. Widgoff, and co-authors, "Charged Pion Production in 147 GeV/c $\pi^-p$ Collisions," B.A.P.S. 20, 546 (1975).

204. M. Heller, A. M. Shapiro, and co-authors, "Study of Double Leading Particle Effects in $\pi^-p$ Interactions at 147 GeV/c," B.A.P.S. 20, 546 (1975).

205. M. Heller, A. M. Shapiro, and co-authors, "Inclusive $\Delta^{++}$ and $\rho^\circ$ Production in 147 GeV/c $\pi^-p$ Interactions," B.A.P.S. 20, 546 (1975).

206. M. Heller, A. M. Shapiro, and co-authors, "The Exclusive Reaction $\pi^-p \to \pi^-p\pi^+\pi^-$ at 147 GeV/c Using the Proportional Wire Hybrid System," B.A.P.S. 20, 546 (1975).

207. D. G. Fong, M. Widgoff, and co-authors, "Strange Particles Produced by $\pi^-p$ Collisions at 147 GeV/c," B.A.P.S. 20, 546 (1975).

208. D. G. Fong, M. Widgoff, and co-authors, "Gamma Ray Production in $\pi^-p$ Reactions at 147 GeV/c," B.A.P.S. 20, 546 (1975).

209. D. G. Fong, M. Heller, A. M. Shapiro, M. Widgoff, and co-authors, "Inelastic 2-Prong Events in 147 GeV/c $\pi^-p$ Collisions," AIP Conference Proceedings of the Seattle Meeting (1975) (to be published).

210. G. T. Chen, C. R. Fletcher, R. E. Lanou, Jr., J. T. Massimo, and co-authors, "Differential Cross Sections for Backward $\pi^+ p \rightarrow n\pi^\circ$ from 2.6 to 8.0 GeV/c," accepted for publication in Physics Letters B (in press) 1975.

211. R. E. Lanou, Jr., J. T. Massimo, R. K. Thornton, and co-authors, "Angular Distributions of $\bar{p}p \rightarrow \pi^\circ\pi^\circ$ and $\bar{p}p \rightarrow \pi^\circ\eta^\circ$ at 1.752 GeV/c," Proceedings of Symposium on Antinucleon-Nucleon Interactions (Prague), edited by L. Montanet, CERN 74-18, 115, 1974.

212. R. E. Lanou, Jr., J. T. Massimo, R. K. Thornton, and co-authors, "Search for Substructure in $\bar{p}p$ Total Cross Section in the 2200 MeV Mass Region," accepted for publication in Physics Letters B (in press) 1975.

213. L. J. Levinson, J. T. Massimo, B. A. Nelson, R. Verdier, "SPEX. A Multitasking System," B.A.P.S. 20, 593 (1975).

214. Anatole M. Shapiro and Robert E. Lanou, Jr., "Progress Report of a Research Program in Experimental High Energy Physics," June 1975.